

RESEARCH ARTICLE

Changes in brown adipose tissue lipid mediator signatures with aging, obesity, and DHA supplementation in female mice

Elisa Félix-Soriano^{1,2}  | Neira Sáinz^{1,2}  | Eva Gil-Iturbe^{1,2}  | María Collantes^{3,4}  |
 Marta Fernández-Galilea^{1,2,4}  | Rosa Castilla-Madrigal^{1,2}  | Lucy Ly⁵ |
 Jesmond Dalli^{5,6}  | María J. Moreno-Aliaga^{1,2,4,7} 

¹Center for Nutrition Research, School of Pharmacy and Nutrition, University of Navarra, Pamplona, Spain

²Department of Nutrition, Food Science and Physiology, School of Pharmacy and Nutrition, University of Navarra, Pamplona, Spain

³Radiopharmacy, Radionanopharmacology and Translational Molecular Imaging Research Group, Clínica Universidad de Navarra, Pamplona, Spain

⁴IdiSNA, Navarra Institute for Health Research, Pamplona, Spain

⁵William Harvey Research Institute, Queen Mary University of London, London, UK

⁶Center for Inflammation and Therapeutic Innovation, Queen Mary University of London, London, UK

⁷CIBER Physiopathology of Obesity and Nutrition (CIBERObn), Instituto de Salud Carlos III (ISCIII), Madrid, Spain

Correspondence

María J. Moreno-Aliaga, Center for Nutrition Research/Department of Nutrition, Food Science and Physiology, School of Pharmacy and Nutrition, University of Navarra, C/Irunlarrea 1, 31008 Pamplona, Spain.
 Email: mjmoreno@unav.es

Funding information

This research was funded by the Government of Spain (MINECO-FEDER, BFU2015-65937-R). CIBER Physiopathology of Obesity and Nutrition (CIBERObn, CB12/03/30002) is also acknowledged. “Juan de la Cierva” grant was provided to M. F.-G. (IJCI-2016-30025). E.F.-S. and E.G.-I received a grant from the Center for Nutrition

Abstract

Brown adipose tissue (BAT) dysfunction in aging and obesity has been related to chronic unresolved inflammation, which could be mediated by an impaired production of specialized proresolving lipid mediators (SPMs), such as Lipoxins-LXs, Resolvins-Rvs, Protectins-PDs, and Maresins-MaRs. Our aim was to characterize the changes in BAT SPMs signatures and their association with BAT dysfunction during aging, especially under obesogenic conditions, and their modulation by a docosahexaenoic acid (DHA)-rich diet. Lipidomic, functional, and molecular studies were performed in BAT of 2- and 18-month-old lean (CT) female mice and in 18-month-old diet-induced obese (DIO) mice fed with a high-fat diet (HFD), or a DHA-enriched HFD. Aging downregulated *Prdm16* and *UCP1* levels, especially in DIO mice, while DHA partially restored them. Arachidonic acid (AA)-derived LXs and DHA-derived MaRs and PDs were the most abundant SPMs in BAT of young CT mice.

Abbreviations: AA, arachidonic acid; ALOX5AP, arachidonate 5-lipoxygenase-activating protein; ALX/FPR2, lipoxin receptor/N-formyl peptide receptor-2; BAT, brown adipose tissue; BMI, body mass index; ChemR23, chemerin Receptor 23; COX-2, cyclooxygenase-2; CT, control; cysLT, cys-Leukotriene; DHA, docosahexaenoic acid; DIO, diet-induced obese; DIOMEG, diet-induced obese+omega-3; EDTA, ethylenediaminetetraacetic acid; EPA, eicosapentaenoic acid; FGF21, fibroblast growth factor 21; GPR120, G protein-coupled receptor 120; GPR32, G protein-coupled receptor 32; hMADS, human adipose tissue-derived mesenchymal stem cells; HDL-cholesterol, high-density lipoprotein cholesterol; HFD, high-fat diet; HRP, horseradish peroxidase; IL, interleukin; LDL-cholesterol, low-density lipoprotein cholesterol; LOX, lipoxygenase; LT, leukotriene; LX, lipoxin; MaR, maresin; MCP-1, macrophage chemoattractant protein-1; MicroPET, micro-positron emission tomography; n-3DPA, omega-3 docosapentaenoic acid; n-3PUFA, omega-3 polyunsaturated fatty acid; PD, protectin; PG, prostaglandin; PGC1 α , peroxisome proliferator-activated receptor γ co-activator 1 α ; PLSDA, partial least squares-discriminant analysis; PMSF, phenylmethylsulfonyl fluoride; PPAR- γ , peroxisome proliferator-activated receptor γ ; PRDM16, PR domain containing 16; Pro-LM, pro-inflammatory lipid mediator; RvD, D-series resolvins; RvE, E-series resolvins; RvT, T-series resolvins; SDS, sodium dodecyl sulfate; SPM, specialized proresolving lipid mediator; SUVmax, maximum standardized uptake value; TBS, tris-buffered saline; TNF- α , tumor necrosis factor- α ; Total-cholesterol, total cholesterol; TRPV1, transient receptor potential vanilloid 1; UCP1, uncoupling protein 1; WAT, white adipose tissue; [¹⁸F]FDG, [¹⁸F]Fluoro-2-deoxy-2-D-glucose.

© 2021 The Authors. The FASEB Journal published by Wiley Periodicals LLC on behalf of Federation of American Societies for Experimental Biology.

This is an open access article under the terms of the Creative Commons Attribution-NonCommercial-NoDerivs License, which permits use and distribution in any medium, provided the original work is properly cited, the use is non-commercial and no modifications or adaptations are made.

Research (University of Navarra). JD is supported by a Sir Henry Dale Fellowship jointly funded by the Wellcome Trust and the Royal Society (grant 107613/Z/15/Z)

Interestingly, the sum of LXs and of PDs were significantly lower in aged DIO mice compared to young CT mice. Some of the SPMs most significantly reduced in obese-aged mice included LXB₄, MaR2, 4S,14S-diHDHA, 10S,17S-diHDHA (a.k.a. PDX), and RvD6. In contrast, DHA increased DHA-derived SPMs, without modifying LXs. However, MicroPET studies showed that DHA was not able to counteract the impaired cold exposure response in BAT of obese-aged mice. Our data suggest that a defective SPMs production could underlie the decrease of BAT activity observed in obese-aged mice, and highlight the relevance to further characterize the physiological role and therapeutic potential of specific SPMs on BAT development and function.

KEYWORDS

aging, brown adipose tissue, DHA, lipidomic, obesity, proresolving lipid mediators

1 | INTRODUCTION

Brown adipose tissue (BAT) is a thermogenic tissue that dissipates energy as heat under certain stimuli, mainly through the uncoupling protein 1 (UCP1).¹ Characterized by multilocular adipocytes with a high mitochondrial content, BAT also plays a relevant role in glucose homeostasis and triglyceride clearance.^{2,3} In the last years, BAT has also emerged as a secretory organ that produces batokines which can influence the activity of other metabolic organs.⁴ Growing evidence supports that BAT mass/activity negatively correlates with BMI, total and visceral adipose tissue, fasting glucose levels, and insulin resistance in rodents and humans.⁵⁻⁹ Therefore, BAT activation has been proposed as a target for the treatment of obesity and related metabolic disorders, including type 2 diabetes and dyslipidaemias.¹⁰

However, BAT activity is gradually lost during the aging process^{8,11} and accordingly, the percentage of adults showing detectable BAT decreases with age.¹² The reduced BAT activation that occurs in aging could favor fat accumulation in older individuals.¹² Therefore, one of the current challenges is to characterize the mechanisms leading to the age-induced reduction of BAT activity, and to discover effective strategies to prevent BAT loss or to reactivate existing BAT depots.¹³

Inflammation seems to be a key process underlying both physiological and pathological processes of aging and obesity.¹⁴ Indeed, both obesity and aging have been identified as chronic, low-grade inflammatory processes. Normal aging leads to a more pro-inflammatory profile that is further accentuated by increased adiposity.¹⁵ White adipose tissue (WAT) dysfunction, characterized by increased expression of pro-inflammatory mediators including interleukin (IL)-1 β , IL-6, tumor necrosis factor- α (TNF- α), and cyclooxygenase-2 (COX-2), and downregulation of the anti-inflammatory peroxisome proliferator-activated receptor γ (PPAR- γ) and adiponectin, contributes to the development of the systemic inflammatory state during aging¹⁶ and obesity.¹⁷ In fact, the concept of “Adipaging” has been proposed, as aging and

obesity share inflammation and other biological hallmarks related to a dysfunctional adipose tissue.¹⁷

Interestingly, BAT seems to be less susceptible to develop local inflammation in response to obesity than WAT.¹⁸ However, strong/chronic pro-inflammatory signals can impair BAT insulin sensitivity and affect its glucose uptake, which is in turn essential for BAT function.¹ Moreover, UCP1-mediated cold-induced thermogenesis is severely impaired in inflamed BAT from diet-induced obese (DIO) mice,¹⁹ and inflammation seems to inhibit the sympathetic tone in BAT through mechanisms yet to be elucidated.¹

In this context, resolution of inflammation is an active process which involves the production of specialized proresolving lipid mediators (SPMs) such as lipoxins (LXs), resolvins (Rvs), protectins (PDs), and maresins (MaRs). Noteworthy, SPMs are decreased in aging in human studies,^{20,21} and the time required for the resolution of inflammation is increased in aged mice.²² Moreover, it has been shown that WAT of obese mice exhibits an impaired production of some SPMs,^{23,24} an event that constitutes one of the earliest alterations in diet-induced inflammation.²⁴ Interestingly, treatment with some of these SPMs (RvD1 and MaR1) or precursors (17-HDHA) reduces WAT inflammation, improves insulin signaling and systemic insulin sensitivity, as well as reduces fatty liver.²⁴⁻²⁷

With this regard, a lipidomic study has revealed a dramatic switch in BAT lipidome toward a WAT-like lipidome after a high-fat feeding period of 20 weeks.²⁸ Regarding SPMs, a recent study has described Lipoxin A4 (LXA₄) and SPMs precursors 18-HEPE, 17-HDHA, and 15-HETE among the main contributors to differentiate BAT from WAT fatty acid metabolomic phenotype.²⁹ However, studies characterizing changes in SPMs levels in BAT during aging and obesity are lacking in the current literature. n-3 polyunsaturated fatty acids (n-3 PUFA) eicosapentaenoic acid (EPA), and docosahexaenoic acid (DHA) serve as substrates for SPMs (Rvs, PDs, and MaRs). Thus, dietary enrichment with n-3 PUFA leads to an increase in SPMs production in

several tissues, including WAT in rodents and humans.^{24,30-33} Furthermore, several studies in cultured adipocytes and in animal models have proposed n-3 PUFA as novel inducers of BAT activity through the stimulation of UCP1, PR domain containing 16 (PRDM16), peroxisome proliferator-activated receptors (PPARs), peroxisome proliferator-activated receptor γ co-activator 1 α (PGC1 α), G protein-coupled receptor 120 (GPR120), and fibroblast growth factor 21 (FGF21).³⁴⁻³⁷

Based in these previous observations, our hypothesis is that the decay in BAT activity that occurs during aging and obesity could be the result of an impaired production of SPMs in this thermogenic tissue. Because n-3 PUFA serve as substrates for the synthesis of SPMs, we propose that long-term dietary supplementation with n-3 PUFA could restore SPMs levels and prevent the alterations in BAT function associated to obesity and aging. Therefore, the aim of this study was to characterize the changes in BAT SPMs signatures in young (2 months old) and aged (18 months old) female mice, as well as their potential associations with BAT function markers, especially in obesogenic conditions and under long-term supplementation with a DHA-enriched diet.

2 | MATERIALS AND METHODS

2.1 | Animal study design

Seven-week-old female C57BL/6J mice were purchased from Harlan Laboratories (Barcelona, Spain) and housed at the animal facilities of the University of Navarra under controlled

conditions ($22 \pm 2^\circ\text{C}$, 12-hour light/12-hour dark cycle; relative humidity $55\% \pm 10\%$). The animal experimental design is available at Figure 1. After 10-days acclimation, 15 animals (young CT, 2 months old) were sacrificed. Next, mice were divided into two experimental groups: a control group (aged CT, 18 months old, $n = 14$) fed a standard control diet up to 18 months of age (20% proteins, 67% carbohydrates, and 13% lipids; Harlan Teklad Global Diets, Harlan Laboratories, Indianapolis, IN, USA); and a diet-induced obese (DIO) group fed with a high-fat saturated diet (High-fat diet, HFD, 20% proteins, 35% carbohydrates, and 45% lipids; Research Diets Inc, New Brunswick, NJ, USA) for 4 months. Afterward, the 6-month-old DIO group was divided into two experimental groups: one continued with the HFD during 12 months (aged DIO, 18 months old, $n = 15$); and the DIO+omega-3 (aged DIOMEG, 18 months old, $n = 11$) that was fed for 12 months with the HFD supplemented with a high DHA fish oil concentrate (SOLUTEX0063TG, containing 683.4 mg DHA/g and 46.7 mg EPA/g, with a total content of 838.9 mg of n-3 PUFA/g as triglycerides, provided by Solutex, Spain), replacing 15% w/w of dietary lipids (Research Diets Inc, New Brunswick, NJ, USA). Because the DHA-rich n-3 PUFA concentrate contained 2 mg/g of mixed tocopherols (Covi-ox T-70EU) to preserve from n-3 PUFA oxidation, the same amount was added to the HFD of the DIO mice that continued with the standard high-fat feeding during this experimental period (from 6 to 18 months). The different HFDs (prepared by Research Diets Inc) were vacuum sealed in 2.5 kg plastic bags and kept frozen (-20°C) until used to avoid rancidity. Specific dietary compositions can be found in a recent manuscript of our group.³⁸

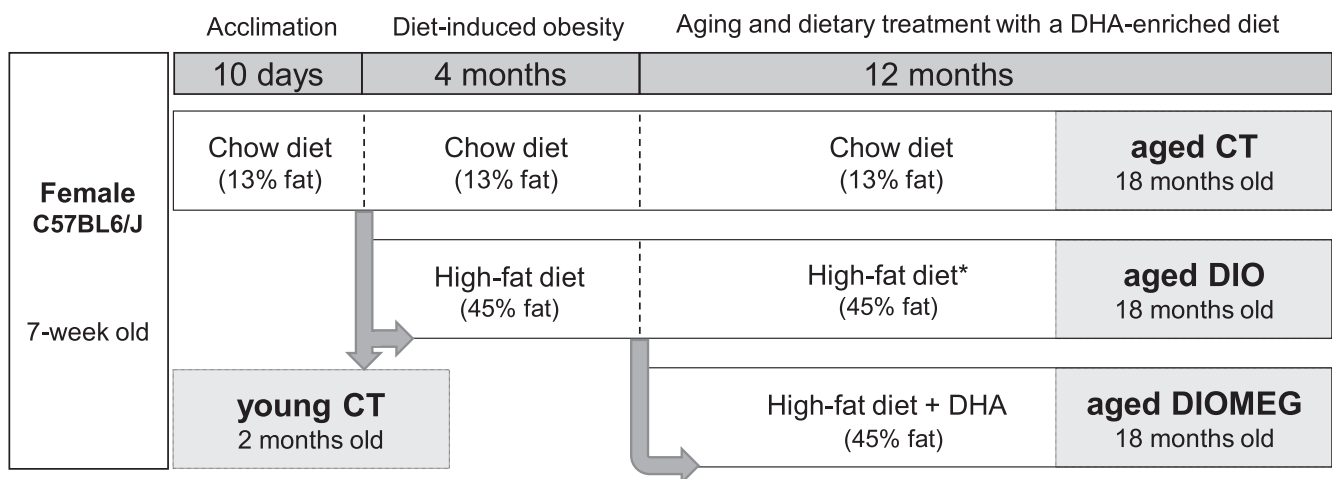


FIGURE 1 Animal experimental design. After 10 days of acclimation, 2-month-old (young CT) mice were sacrificed. The rest of mice were divided into two groups, one fed with a standard diet (CT) and other fed with a high-fat diet (HFD) for 4 months to induce obesity (DIO). These 6-month-old DIO mice were divided into two subgroups and aged up to 18 months: the aged DIO group was fed with the HFD* and the aged DIOMEG group was fed with a DHA-enriched HFD. The HFD* (from 6 to 18 months) was formulated with the same amount of tocopherol mix contained in the DHA-enriched HFD to preserve from oxidation. An aged CT group fed with the standard diet up to 18 months was also included. Body composition was determined in young CT and aged (CT, DIO and DIOMEG) groups. Serum and adipose tissue samples were also collected, and BAT was characterized (by morphological, gene and protein expression, and lipidomic analysis). BAT activity was evaluated by MicroPET analysis

All experimental groups were fed ad libitum. Animals were controlled for weight and food intake 3 days/week during the whole experiment. At 2 and 18 months of age, animals underwent body composition analyses. After an overnight fast, fat depots (interscapular BAT, subcutaneous inguinal, mesenteric, gonadal, and retroperitoneal WAT) were collected, weighted, and frozen at -80°C . Total WAT weight was estimated as the weight sum of inguinal, gonadal, retroperitoneal, and mesenteric white fat depots. BAT samples for histological analysis were also obtained, and frozen BAT samples were used for lipidomic, protein, and gene expression analyses. Blood samples were collected, and serum was obtained and frozen at -80°C for biochemical determinations. At 2 and 18 months of age, a subset of five animals per group underwent MicroPET imaging analyses for in vivo BAT activity determination.

The study was designed in female mice since sex-dependent inactivation of thermogenesis in BAT has been proposed as one of the mechanisms favoring fat accumulation, and underlying the higher propensity for obesity under hypercaloric conditions in female rats as compared to males.³⁹ Moreover, BAT thermogenic activity was found to be depressed in female rats during caloric restriction as compared to males.⁴⁰ Furthermore, a reduced norepinephrine turnover rate in cold-induced thermogenesis has also been described in older female rats, but not in male,⁴¹ suggesting a more impaired thermogenic response to diet and in aging in female than in male rodents.

All experiments were performed according to national animal care guidelines, with the approval of the Ethics Committee for Animal Experimentation of the University of Navarra (protocol no. 113-15) in accordance with the EU Directive 2010/63/EU.

2.2 | Body composition analyses

Before the sacrifice, whole-animal body composition was measured in live conscious animals with nuclear resonance technology (EchoMRI-100-700; Echo Medical Systems, Houston, TX, USA) as previously described.⁴²

2.3 | Biochemical analysis

Serum biochemical analyses were performed after a 12 hours fasting period. Glucose, total cholesterol (total chol), HDL-cholesterol (HDL-chol), triglycerides, and β -hydroxybutyrate serum levels were determined using a Pentra C200 auto analyzer (HORIBA ABX, Madrid, Spain), following the manufacturer's instructions. LDL-cholesterol (LDL-chol) values were calculated using the Friedewald equation ($\text{LDL cholesterol} = \text{Total-cholesterol} - \text{HDL-cholesterol} - \text{TG}/5$). Insulin levels were determined with a commercially available

ELISA kit (Mercodia, Uppsala, Sweden), according to the supplier's guidelines.

2.4 | In vivo BAT activity by micro-positron emission tomography (MicroPET) assay

In vivo BAT activity was estimated by MicroPET imaging using the glucose analog [^{18}F]Fluoro-2-deoxy-2-D-glucose ([^{18}F]FDG). Studies were performed in a small animal Philips Mosaic tomograph (Cleveland, OH, USA) at the MicroPET Unit of Clínica Universidad de Navarra.⁴³ On the day of each PET study, mice were pre-exposed to cold stimulation for 1 hour. [^{18}F]FDG (10.1 ± 0.9 MBq) was injected through the tail vein 1 hour before PET scanning. Mice were under anesthesia throughout the PET acquisition procedure. For the assessment of [^{18}F]FDG uptake, all studies were exported and analyzed using the PMOD software (PMOD Technologies Ltd., Adliswil, Switzerland). Images were expressed in standardized uptake value (SUV) units, using the formula $\text{SUV} = [\text{tissue activity concentration (Bq/cm}^3\text{)}/\text{injected dose (Bq)}] \times \text{body weight (g)}$. For semi-quantitative analysis, [^{18}F]FDG uptake by BAT was evaluated drawing volume-of-interest (VOIs) on coronal PET images including the interscapular BAT. From each VOI, maximum voxel intensity within the VOI (SUVmax) was recorded.

Ex vivo quantification of [^{18}F]FDG uptake in BAT depots was also measured. For this purpose, interscapular BAT depots were extracted immediately after PET imaging. Tissues were weighed and measured for [^{18}F]FDG activity on a high-energy γ counter. Uptake levels were expressed as percentage of injected dose per gram of tissue.

2.5 | Histological analysis of BAT

BAT samples of the four experimental groups were fixed in 3.7%–4.0% neutral formalin (pH 7.4) for 24 hours, dehydrated with 70% ethanol, and embedded in paraffin. Five micrometers sections were deparaffinized and stained with hematoxylin-eosin (H&E). BAT images (magnification 40 \times) were taken with an Olympus inverted microscope (CKX31SF, Olympus Corp., Tokyo, Japan) coupled to an Olympus C-5060 WIDE ZOOM digital compact camera (Olympus Corp.). Mean lipid droplet surface in BAT H&E-stained samples was quantified with ImageJ 2.0 imaging suite (US National Institutes of Health, Bethesda, MD, USA).

2.6 | BAT lipid mediator profiling

All samples were extracted using solid-phase extraction columns as previously described.^{44,45} Prior to sample

extraction, deuterated internal standards, representing each region in the chromatographic analysis (500 pg each) were added to facilitate quantification in 1 mL of methanol. Samples were kept at -20°C for a minimum of 45 minutes to allow protein precipitation. Supernatants were subjected to solid-phase extraction, methyl formate and methanol fractions were collected, brought to dryness, and suspended in phase (methanol/water, 1:1, vol/vol) for injection on a Shimadzu LC-20CE HPLC and a Shimadzu SIL-20AC autoinjector (Shimadzu Corp., Kyoto, Japan), paired with a QTrap 6500+ (Sciex, Warrington, UK). For identification and quantitation of products eluted in the methyl formate an Agilent Poroshell 120 EC-C18 column (100 mm \times 4.6 mm \times 2.7 μm , Agilent Technologies, Santa Clara, CA, USA) was kept at 50°C and mediators eluted using a mobile phase consisting of methanol-water-acetic acid of 20:80:0.01 (vol/vol/vol) that was ramped to 50:50:0.01 (vol/vol/vol) over 0.5 minutes and then, to 80:20:0.01 (vol/vol/vol) from 2 minutes to 11 minutes, maintained till 14.5 minutes and then, rapidly ramped to 98:2:0.01 (vol/vol/vol) for the next 0.1 minutes. This was subsequently maintained at 98:2:0.01 (vol/vol/vol) for 5.4 minutes, and the flow rate was maintained at 0.5 mL/min. QTrap 6500+ was operated using a multiple reaction monitoring method coupled with information-dependent acquisition and enhanced production scan. In the analysis of peptide-lipid-conjugated mediators eluted in the methanol fraction, Agilent Poroshell 120 EC-C18 column (100 mm \times 4.6 mm \times 2.7 μm , Agilent Technologies) was kept at 50°C and mediators were eluted using a mobile phase consisting of methanol-water-acetic acid at 55:45:0.1 (vol/vol/vol) over 5 minutes, that was ramped to 80:20:0.1 (vol/vol/vol) for 2 minutes, maintained at 80:20:0.1 (vol/vol/vol) for the next 3 minutes, and ramped to 98:2:0.1 (vol/vol/vol) over 3 minutes. This was kept at 98:2:0.1 (vol/vol/vol) for 3 minutes. A flow rate of 0.60 mL/min was used throughout the experiment. QTrap 6500+ was operated in positive ionization mode using multiple reaction monitoring (MRM) coupled with information-dependent acquisition and enhanced production scan. Each LM was identified using established criteria, including matching retention time to synthetic and authentic materials and at least six diagnostic ions. Calibration curves were obtained for each using synthetic compound mixtures at 0.78, 1.56, 3.12, 6.25, 12.5, 25, 50, 100, and 200 pg that gave linear calibration curves with an r^2 values of 0.98-0.99.⁴⁶

2.7 | Protein isolation and Western Blot analyses

BAT samples were homogenized by sonication (SONOPULS Ultrasonic homogenizer HD 3100, Bandelin, Berlin, Germany) two times for 10 seconds each in 200 μL lysis

buffer (8 mmol/L NaH_2PO_4 , 42 mmol/L Na_2HPO_4 , 1% sodium dodecyl sulfate (SDS), 0.1 mol/L NaCl, 0.1% NP40, 1 mmol/L NaF, 10 mmol/L sodium orthovanadate, 2 mmol/L phenylmethylsulfonyl fluoride (PMSF), 10 mM ethylenediaminetetraacetic acid (EDTA), and 1% protease inhibitor cocktail 1 (Millipore Sigma, St. Louis, MO, USA)). Then, samples were centrifuged at 13 000 rpm for 15 minutes to obtain the supernatant fraction containing the proteins. The protein extracts were quantified with the BCA protein assay kit (Thermo Fisher Scientific, Waltham, MA, USA) to determine their concentration.⁴⁷

Protein extracts (15-20 μg) were resolved by electrophoresis on 12% SDS-polyacrylamide gels and then, electroblotted onto a polyvinylidene difluoride membrane (Hybond P; GE Healthcare, Chicago, Ill., USA), which was blocked in TBS-Tween 1X buffer (TBS-T 1X) with 10% of milk (Nestle, Switzerland) for 1 hour at room temperature. Then, primary antibody anti-UCP1 (rabbit, Abcam, Cambridge, UK), was used at 1:1000 overnight at 4°C . After incubation, goat anti-rabbit IgG peroxidase-conjugated (HRP) secondary antibody (Cell Signaling Technology, MA, USA) was used at 1:10 000 for 1 hour at room temperature. The immunoreactive proteins were detected with enhanced chemiluminescence (Thermo Fisher Scientific) and quantified by densitometry analysis (LI-COR Biosciences, Lincoln, NE, USA). The results are expressed in relation to the young CT group value, which was set to 100%.

2.8 | Gene expression by qRT-PCR

Total RNA from BAT depots was extracted with QIAzol Lysis reagent (Qiagen, Hilden, Germany). After quality and concentrations were measured (Nanodrop Spectrophotometer ND1000, Thermo Fisher Scientific), RNA (2 μg) was incubated with DNase I (Life Technologies, Carlsbad, CA, USA) for 30 minutes at 37°C . Retrotranscription to cDNA was performed using High-Capacity cDNA Reverse Transcription (Applied Biosystems, Foster City, CA). Real-time PCR was performed using the Touch Real-Time PCR System (C1000 + CFX384, BIO-RAD, Hercules, CA, USA). Gene expression was analyzed using Power SYBR Green PCR (Bio-Rad, München, Germany). Primer-Blast software (National Center for Biotechnology Information, Bethesda, MD, USA (<https://www.ncbi.nlm.nih.gov/tools/primer-blast/>)) was used to design the following primers: *Ccl2* (forward: 5'-AGCACCCAGCCAACTCTCACT-3'; reverse: 5'-TCATTGGGATCATCTTGCTG-3'), *Fgf21* (forward: 5'-CCTCTAGGTTTCTTTGCCAACAG-3', reverse: 5'-AAGCTGCAGGCCTCAGGAT-3'), *Ill10* (forward: 5'-AAGGAGTGGAGCAGGTGAA-3', reverse: 5'-CCAGCAGACTCAATACACAC-3'), *Il4* (forward: 5'-ACAGGAGAAGG GACGCCAT-3', reverse: 5'-GAAGCCCTACAGACGAGCTCA-3'), *Prdm16* (forward: 5'-CAGCACGGTGAAGCCAT

TC-3', reverse: 5'-GCGTGCATCCGCTTGTG-3'), and *36b4* (forward: 5'-CACTGGTCTAGGACCCGAGAAG-3', reverse: 5'-GGTGCCTCTGGAGATTTTCG-3'). Relative gene expression was determined by the $2^{-\Delta\Delta CT}$ method⁴⁸ after internal normalization to *36b4*.

2.9 | Statistical analysis

Statistical analyses were performed using one-way ANOVA or Kruskal-Wallis test followed by post hoc test for multiple groups comparisons, and unpaired Student's *t* or Mann-Whitney's *U* test for direct comparisons between two groups after testing the normality with the Kolmogorov-Smirnov and Shapiro-Wilk tests. GraphPad Prism 9 software (La Jolla, CA, USA) and Stata 14 (Stata, Collage Station, TX, USA) were used for statistical analysis. Results were expressed as mean \pm SEM and differences were considered significant at a *P* value $< .05$.

For lipid mediator analyses by PLSDA, its Scores Plot and VIP Scores, as well as the heatmap of lipid mediator's distribution across the four experimental groups and the Pearson's correlations with BAT genes, MetaboAnalyst 4.0 (University of Alberta, Edmonton, AB, Canada) was used.

3 | RESULTS

3.1 | Body composition, fat depots weight, and serum biomarkers of glucose and lipid metabolism

Table 1 shows body composition data and serum glucose and lipid metabolism biomarkers of young (2 months old) and aged (18 months old) mice fed with a control diet (CT) or a HFD without (DIO) or with DHA (DIOMEG). As expected, the aged CT mice exhibited increased body weight,⁴⁷ fat mass, as well as hyperglycemia and higher levels of total and LDL-chol as compared to young CT mice. The metabolic changes that occurred during aging were aggravated in the aged DIO mice, which accumulated more fat and exhibited a worsened hyperglycemia, hyperinsulinemia, and dyslipidemia (Table 1). Chronic feeding with the DHA-rich diet (aged DIOMEG group) tended to reduce body weight^{38,47} and fat accumulation especially in the white adipose depots, in parallel with improved total chol, LDL-chol, and the atherogenic index LDL-chol/HDL-chol compared to the aged DIO group, without significantly affecting fasting glucose and insulin levels (Table 1). Thus, long-term feeding with a DHA-enriched HFD improved lipid serum profile as compared to aged DIO animals but had no significant effects on body composition and glucose metabolism biomarkers as compared to aged DIO mice.

3.2 | Aging-induced morphological, transcriptomic, and functional changes in BAT of lean, obese, and DHA-supplemented obese mice

In order to study the effects of aging and obesity and the long-term DHA supplementation on BAT biology, the changes on BAT morphology and on the expression of genes/proteins related to BAT development, function, and inflammatory status were investigated. Aging-induced lipid accumulation also in brown adipocytes, as revealed by the increased weight and the histological images of BAT depots in young vs aged CT mice. A dramatic BAT hypertrophy accompanied by the appearance of unilocular adipocytes was observed in the aged DIO group, which was partly attenuated in the aged DIOMEG group, although no significant differences were reached neither in BAT weight nor in adipocyte lipid droplets size (Table 1, Figure 2A, Figure S1).

We further evaluated if the hypertrophy of BAT associated to obesity and aging occurred alongside with an altered expression of genes and proteins related to BAT development and function. Our data show that the levels of UCP1, the main responsible of BAT thermogenesis, was significantly reduced in aged CT as compared to young CT mice. Such reduction tended to be more pronounced in aged DIO mice. Noteworthy, the HFD supplementation with DHA restored UCP1 expression in BAT of aged obese mice (Figure 2B). A similar pattern was observed for *Prdm16*, which is required for the maintenance and function of brown adipocytes in adult mice.⁴⁹ Indeed, *Prdm16* mRNA expression was reduced with aging and worsened by obesity, but partially recovered in the aged DIOMEG group (Figure 2C). Moreover, *fibroblast growth factor 21 (Fgf21)*, which has been also related to brown fat activation,³⁶ was decreased with aging in BAT of aged CT mice but increased in BAT of aged DIO mice. Increased FGF21 has been related to resistance to its action and as a mechanism to counteract the increased inflammatory/oxidative stress state associated to obesity.⁵⁰ Interestingly, *Fgf21* mRNA levels were normalized in the aged DIO mice fed with the DHA-enriched diet (Figure 2C). In line with this result, the mRNA levels of the pro-inflammatory marker *Ccl2* (encoding for macrophage chemoattractant protein 1, MCP-1) were increased by aging (aged CT) and further augmented by obesity (aged DIO), but normalized to those of the aged CT mice with the DHA treatment in the aged DIOMEG group. In contrast, the levels of *Il4*, which induces M2 macrophages polarization,⁵¹ were decreased in the aged DIO group as compared with age-matched CT mice, but dietary DHA was not able to rescue this drop in *Il4* mRNA levels (Figure 2C). Strikingly, an upregulation of the anti-inflammatory cytokine *Il10* was observed during aging and especially in obese mice, which was reversed in the obese

TABLE 1 Effects of aging on body composition, white and brown adipose tissue weights, and serum biomarkers of glucose and lipid metabolism in young and aged lean (CT) and aged obese mice fed with a diet rich in saturated fat (DIO) or a diet enriched in DHA (DIOMEG)

	Young		Aged		
	CT		CT	DIO	DIOMEG
Fat mass (%)	13.19 ± 0.59		29.82 ± 1.89 ^{***}	53.44 ± 1.69 ^{***,###}	50.45 ± 1.35 ^{***,###}
BAT (g)	0.06 ± 0.00		0.09 ± 0.01 ^{***}	0.26 ± 0.03 ^{***,###}	0.20 ± 0.01 ^{***,###}
WAT (g)	0.40 ± 0.03		1.79 ± 0.19 ^{***}	8.15 ± 0.81 ^{***,###}	5.66 ± 0.16 ^{**,#}
Triglycerides (mg/dL)	52.50 ± 6.70		58.29 ± 3.26	66.67 ± 3.94	61.50 ± 6.25
Total chol (mg/dL)	66.75 ± 4.85		98.86 ± 7.05 [*]	134.78 ± 7.33 ^{**,#}	90.75 ± 9.72 [‡]
LDL-chol (mg/dL)	21.95 ± 3.42		38.65 ± 3.72 [*]	67.48 ± 5.07 ^{**,#}	27.06 ± 3.76 ^{‡‡}
HDL-chol (mg/dL)	34.30 ± 2.54		48.55 ± 3.37 [*]	53.93 ± 3.04 ^{**}	51.39 ± 5.46
LDL-chol/HDL-chol	0.64 ± 0.08		0.79 ± 0.03	1.25 ± 0.07 ^{**###}	0.52 ± 0.03 ^{###,‡‡}
β-Hydroxybutyrate (mmol/L)	1.53 ± 0.34		1.31 ± 0.15	1.32 ± 0.11	1.35 ± 0.31
Glucose (mmol/L)	4.89 ± 0.64		5.84 ± 0.49 [*]	7.61 ± 0.50 ^{**,#}	7.79 ± 0.68 ^{**,#}
Insulin (mU/L)	2.99 ± 0.21		2.90 ± 0.06	4.43 ± 0.33 ^{**###}	3.61 ± 0.32 [#]

Note: Data are expressed as mean ± SEM. Fat mass (%) corresponds to body composition analysis performed in non-fasted mice. BAT and WAT weights and biochemical analysis are from overnight fasted mice. (n = 5-10).

P* < .05; *P* < .01; ****P* < .001 vs young CT group.

#*P* < .05; ##*P* < .01; ###*P* < .001 vs aged CT group.

‡*P* < .05; ‡‡*P* < .01 vs aged DIO group.

mice receiving the DHA-supplemented diet (Figure 2C). Taken together, all these data suggest that DHA was able to reverse the detrimental gene and protein expression pattern in BAT induced by aging and further worsened by obesity, even in the absence of major morphological changes.

3.3 | Effects of aging, obesity, and DHA-supplementation on BAT lipid mediators' signature

Because lipid mediators have been considered as key regulators of BAT function,^{52,53} we next aimed to characterize the lipid mediator signature of BAT in young and aged mice as well as the changes induced by long-term feeding with saturated fat or n-3 PUFA-enriched fat. Lipid mediator profiling of the n-3 Docosapentaenoic Acid (DPA), EPA, DHA, and Arachidonic acid (AA)-derived bioactive metabolomes demonstrated that the AA-derived LXs are the most abundant SPMs, followed by DHA-derived MaRs and PDs, in BAT of young female mice housed at 22°C (Figure 3). Figure S2 shows a heatmap of all lipid mediators analyzed, as well as the sum of each lipid mediator's classes in the young and aged lean (CT), aged obese (DIO), and aged obese+DHA (DIOMEG) groups. Figure 4A shows the PLSDA analysis of lipid mediators' concentrations in BAT of the four experimental groups. Colored ellipse areas display the 95% confidence region. As shown by the Scores Plot, the young and aged CT groups shared more similarities in lipid mediators'

distribution than the aged DIO group, suggesting that the differences in lipid mediators induced by aging were aggravated by the diet-induced obesity. Moreover, the aged DIOMEG group was clearly differentiated from the rest of the groups, despite being fed with a diet providing the same fat amount but partially replaced by a high DHA n-3 PUFA concentrate. Moreover, the PLSDA VIP scores revealed that mediators from the Rvs and MaRs families were predominant among the main 15 mediators contributing to such differences between groups (Figure 4B). Furthermore, the analyses of the total SPMs abundance between the four experimental groups showed that the aged DIO group displayed significantly lower SPMs levels when compared to the young CT group. Noteworthy, n-3 PUFA supplementation was able to significantly increase SPMs levels in the DIOMEG group compared not only to the aged CT and DIO groups, but also to the young CT group (Figure 4C).

We further aimed to characterize the contribution of the n-3 DPA, DHA, EPA, and AA-derived SPMs to the observed effects in BAT of the obese-aged mice and after the long-term feeding with the DHA-enriched HFD. Interestingly, only the sum of PDs and LXs was significantly lower in the aged DIO group than in the young CT group (Figure 4D). The reduction in LXs levels found in the DIO-aged mice compared to CT young mice did not improve with n-3 PUFA supplementation, likely because LXs are produced from AA. In contrast, the sum of each n-3 DPA, DHA, and EPA-derived SPMs classes was significantly elevated in those mice fed with the DHA-rich HFD, reaching levels significantly higher than those

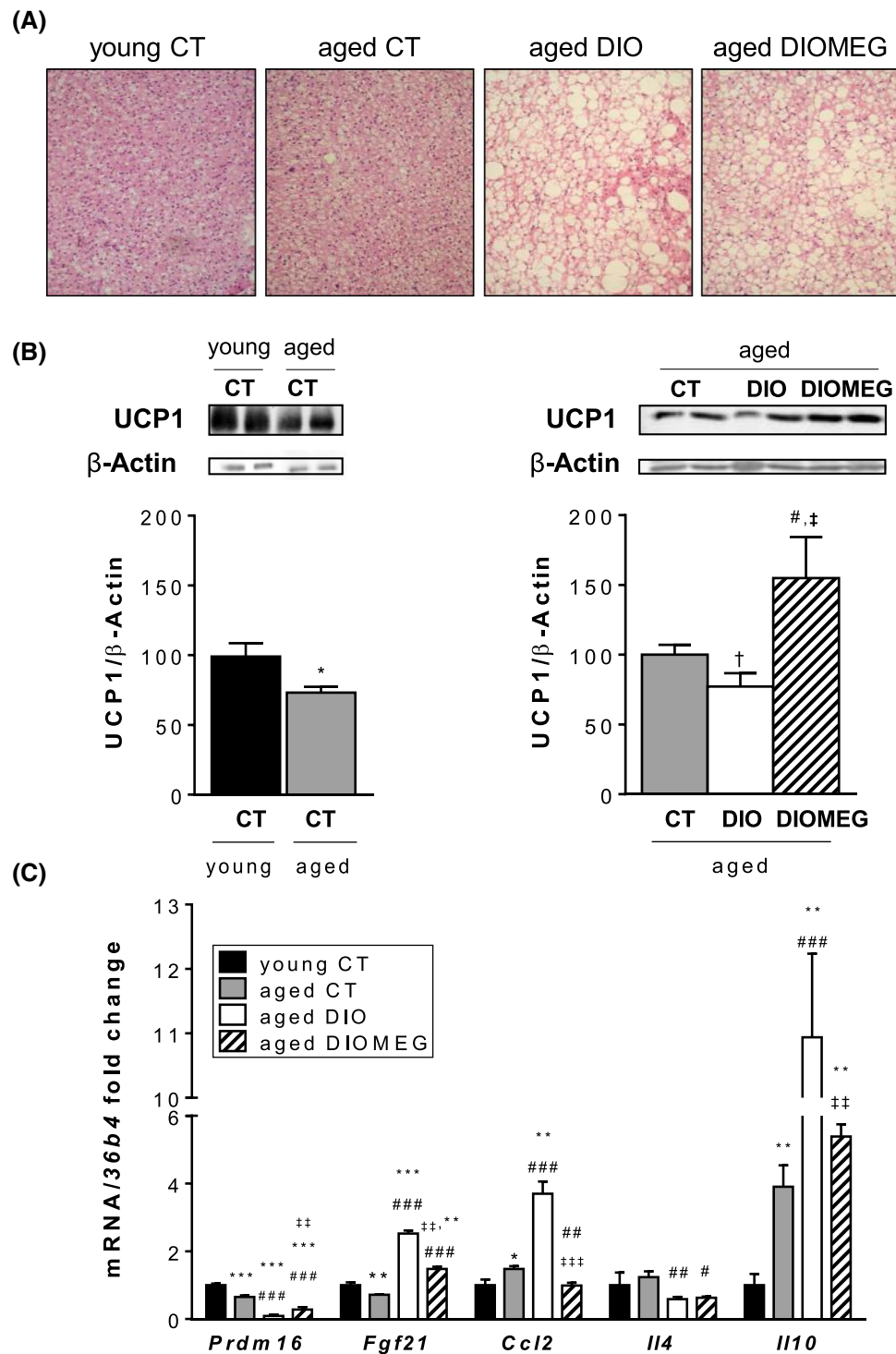


FIGURE 2 Differential effects of aging on BAT morphology, gene, and protein expression in young and aged lean (CT), as well as in obese female mice chronically fed with a HFD rich in saturated fat (DIO) or with a DHA-enriched HFD (DIOMEG) at 18 months of age. A, Representative BAT histology images. B, UCP1 protein levels in BAT of young vs aged control mice (CT, left panel) and in BAT of aged CT, DIO, and DIOMEG mice (right panel). Representative western blot (top panel) and densitometry analysis (bottom panel) of UCP1. Band densities of UCP1 were normalized to β -actin. C, mRNA levels of genes involved in BAT development, function, and inflammation. Data are expressed as mean \pm SEM. (n = 5-10). * $P < .05$, ** $P < .01$, *** $P < .001$ vs young CT group; # $P < .05$, ## $P < .01$, ### $P < .001$ vs aged CT group; † $P < .05$, ‡ $P < .01$, ‡‡ $P < .001$ vs aged DIO group; † $P = .071$ vs aged CT group

FIGURE 3 Abundance of AA, DHA, n-3 DPA, and EPA-derived specialized proresolving lipid mediators (SPMs) in BAT from young female mice (2 months of age). (n = 5). ****P* < .001 vs LXs; #*P* < .05, ##*P* < .01 vs MaRs

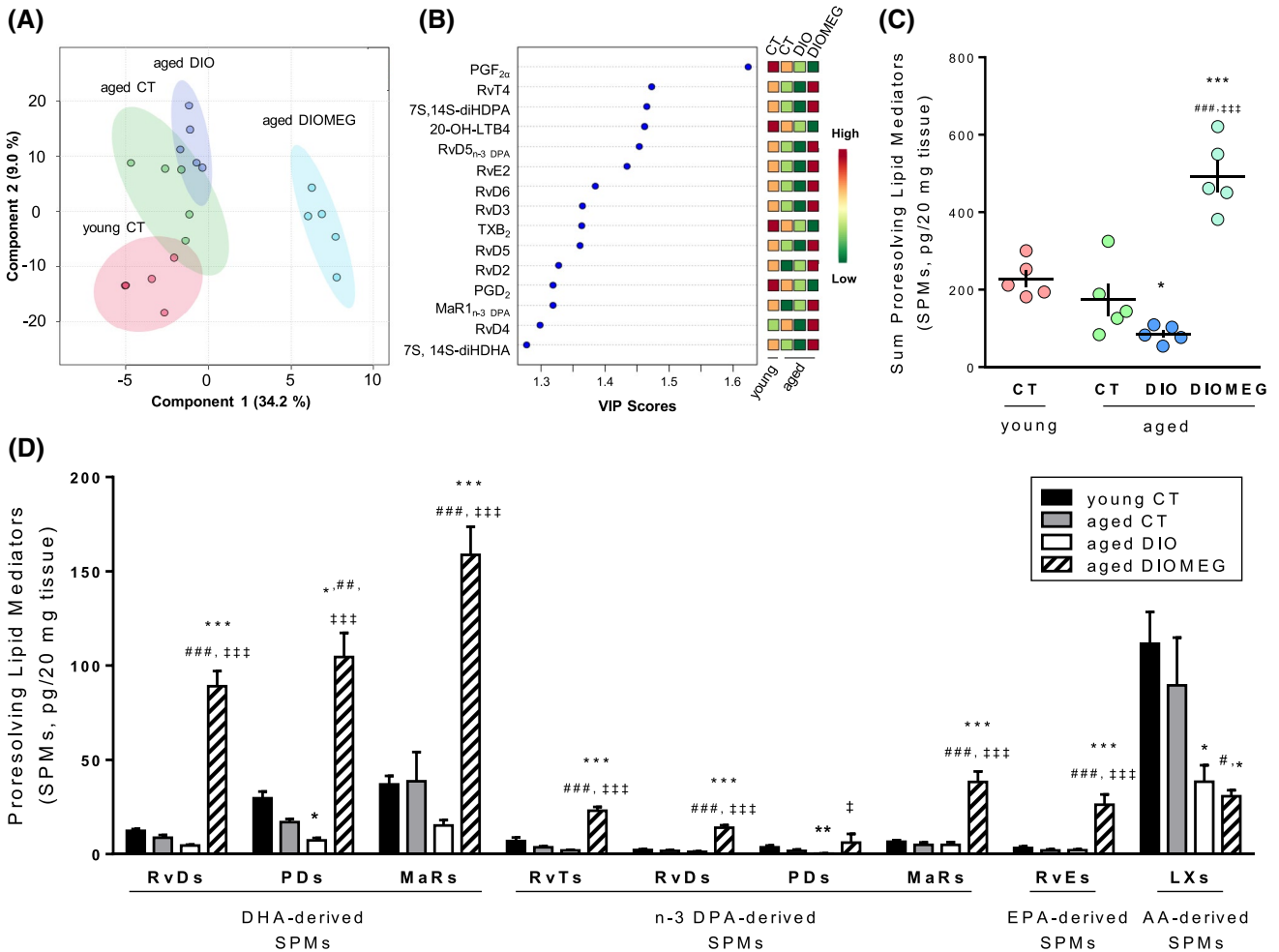
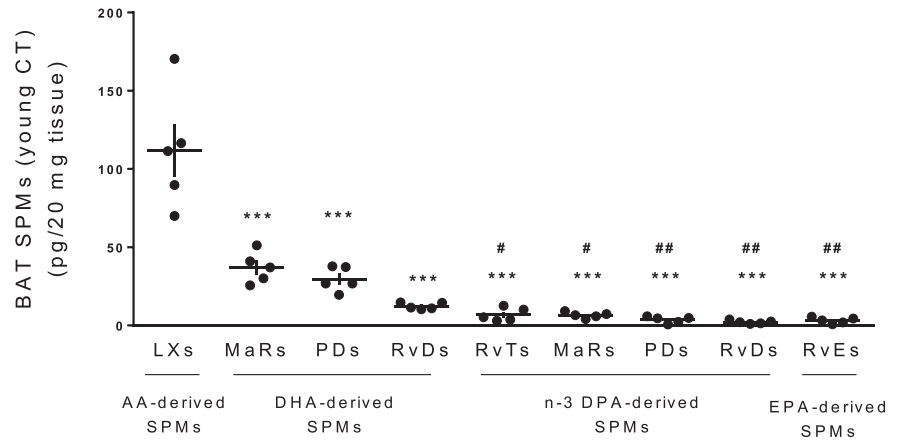


FIGURE 4 Changes in BAT lipid mediators profile induced by aging, obesity, and dietary DHA supplementation. A, PLSDA analysis of lipid mediator concentrations in BAT of the four experimental groups. Colored spherical areas display the 95% confidence region. B, Vip Scores of the 15 lipid mediators contributing more to the separation between groups in the PLSDA model. C, Sum of specialized proresolving lipid mediators (SPMs) showing reduced levels in aged (18 months old) DIO mice but not in DIOMEg mice. D, Graph bar showing the differential distribution of the different types of SPMs (DHA, n-3 DPA, EPA, and AA-derived) in the four groups of study. Data are expressed as mean ± SEM. (n = 5). **P* < .05, ***P* < .01, ****P* < .001 vs young CT group; #*P* < .05, ##*P* < .01, ###*P* < .001 vs aged CT group; †*P* < .05, ‡*P* < .001 vs aged DIO group

found even in young CT mice (Figure 4D). Our next step was to analyze the changes in individual n-3 DPA, DHA, and EPA-derived lipid mediators, to identify those with most relevance/contribution to the reduced levels of SPMs observed

in aged obese animals and those that were most markedly stimulated by n-3 PUFA supplementation. Among them, MaR2 and 4S,14S-diHDHA (Figure 5A), 10S,17S-diHDHA, 17R-PD1, PD2_{n-3 DPA} and 10S,17S-diHDPA (Figure 5B), and

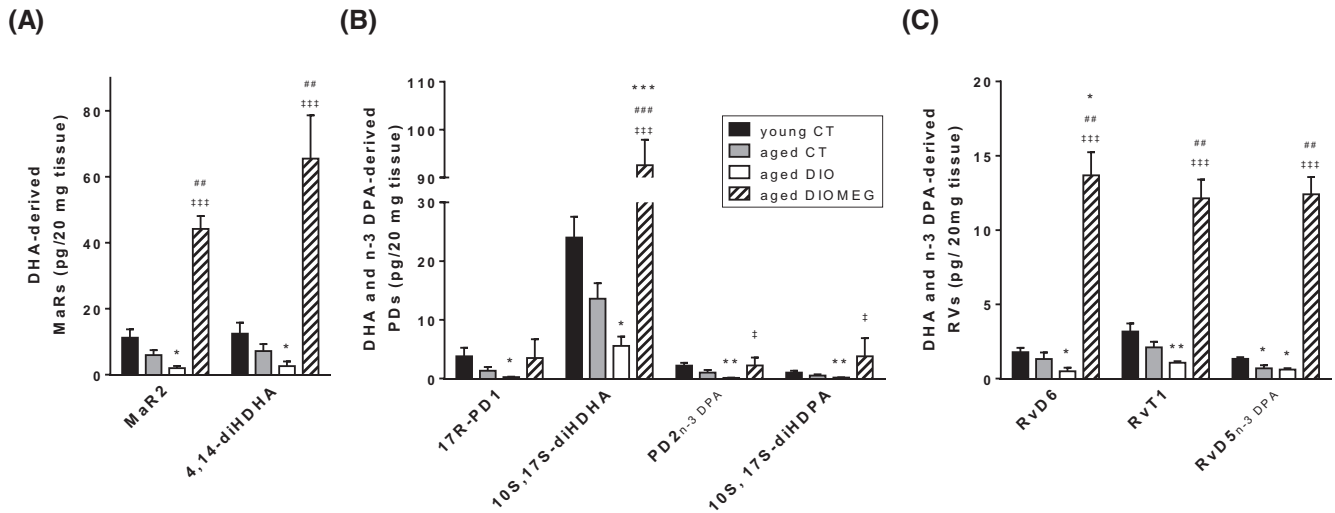


FIGURE 5 Quantification of principal changes induced by aging, obesity, and dietary DHA supplementation on BAT-specific SPMs and lipid intermediates of the DHA and/or n-3 DPA-derived Maresins (MaRs, A), Protectins (PDs, B), and Resolvins (Rvs, C) pathways. Data are expressed as mean \pm SEM. (n = 5). * P < .05, ** P < .01, *** P < .001 vs young CT group; ## P < .01, ### P < .001 vs aged CT group; ‡ P < .05, ‡‡ P < .001 vs aged DIO group

RvD6, RvT1, and RvD5_{n-3 DPA} (Figure 5C) were the most decreased by the combination of chronic high-fat feeding and aging, as revealed by the comparison of the aged DIO to the young CT group. More information concerning the changes in other SPMs and lipid intermediates of the DHA and n-3 DPA-derived MaRs, PDs, Rvs pathways can be found in Figure S3A-C. It is worth mentioning that E-series Rvs concentrations were not affected by either age or obesity (Figure S3D). Concerning the changes induced by long-term supplementation with the DHA-enriched diet on specific SPMs, our data revealed that almost all DHA and n-3 DPA-derived MaRs (MaR1, MaR2, 4S,14S-diHDHA, 7S,14S-diHDHA, MaR2_{n-3 DPA}, and 7S,14S-diHDPA), PDs (PD1, 10S,17S-diHDHA, 17R-PD1, PD2_{n-3 DPA}, and 10S,17S-diHDPA), and Rvs (RvD1-6, 17R-RvD3, RvT1 and RvT4, and RvD1_{n-3 DPA}, RvD2_{n-3 DPA}, and RvD5_{n-3 DPA}) were higher in the aged DIOMEG group when compared to the aged DIO group (Figure 5A-C, Figure S3A-C). Regarding EPA-derived Rvs, RvE2 and RvE3, but not RvE1, were markedly increased in the aged DIOMEG group (Figure S3D). A moderate increase in some EPA-derived Rvs could be expected, as the DHA-rich n-3 PUFA concentrate also contained a small amount of EPA.

The analyzed AA-derived pro- and anti-inflammatory lipid mediators are shown in Figure 6. Our data revealed a significant decrease in LXA₄, LXB₄, and 15-epi-LXA₄ in BAT of aged DIO mice compared to young CT mice (Figure 6A). Another relevant finding was the decrease in PGF_{2 α} observed in BAT of aged mice (both CT and DIO) when compared with young mice (Figure 6B). A reduction in LTC₄ and 20-OH-LTB₄ was also observed in aged DIO mice as compared to the young CT mice (Figure 6C). No

other significant changes were observed in AA-derived lipid mediators because of aging and/or obesity. Regarding the effects of the DHA-rich HFD, PGE₂ and PGF_{2 α} were decreased (Figure 6B), while LTC₄ was increased (Figure 6C), in the aged DIOMEG group as compared to the aged DIO group.

In summary, aging and obesity rather than aging alone had lowering effects on SPMs abundance, while few pro-inflammatory lipid mediators were significantly affected by these conditions. The DHA-rich HFD reverted this decrease in several of the DHA, n-3 DPA, and EPA-derived SPMs, without restoring the AA-derived SPMs.

3.4 | Correlations between BAT genes and lipidomics

With the aim to characterize the potential relationship between the levels of lipid mediators and the mRNA levels of genes involved in BAT development, function, and inflammatory status, Pearson's correlations were carried out. Figure 7 shows the heatmap of correlations between BAT genes (*Prdm16*, *Fgf21*, *Ccl2*, *Il4*, and *Il10*) and each lipid mediator/pathway marker identified, or with sums of the different lipid mediator's families, considering all experimental groups of the study. *Prdm16* gene expression positively correlated with the sum of LXs, as well as with some individual lipid mediators from the LXs family (LXB₄, 15-epi-LXA₄, and 15-epi-LXB₄). A positive correlation was also found with LTC₄ and 5S,12S-diHETE (LTB₄ pathway marker), and with the sums of LTBs and cysLTs. These apparently contradictory results could be explained by the fact that these lipid mediators are all derived from

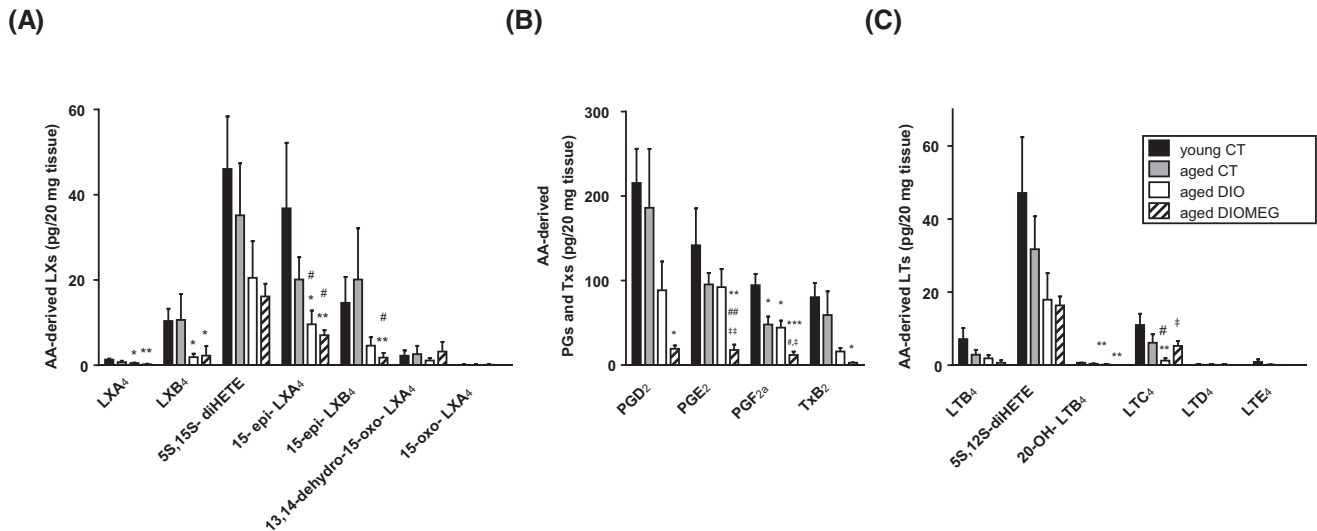


FIGURE 6 Characterization of changes in specific AA-derived lipid mediators involved in the Lipoxins (LXs, A), Prostaglandins and Thromboxanes (PGs and TXs, B) and Leukotrienes (LTs, C) pathways in BAT of female mice induced by aging, obesity, and dietary DHA supplementation. Data are expressed as mean \pm SEM. (n = 5). * $P < .05$, ** $P < .01$, *** $P < .001$ vs young CT group; # $P < .05$, ## $P < .01$ vs aged CT group; ‡ $P < .05$, ‡‡ $P < .01$ vs aged DIO group

the lipoxygenase (LOX) AA-pathway. Moreover, *Prdm16* correlated with 4S,14S-diHDHA, pathway marker of the DHA-derived MaRs.

Regarding *Fgf21*, its mRNA levels negatively correlated with some individual AA-derived pro-inflammatory lipid mediators (LTC_4 , PGD_2 , and TxB_2), and with the sum of LTBs, $cysLTs$, TXs, and the total of pro-inflammatory lipid mediators (Pro-LMs). Nevertheless, a negative correlation was observed for 15-epi- LXA_4 , 15-epi- LXB_4 , and for the sum of LXs, suggesting a role for both pro-inflammatory and proresolving AA-derived lipid mediators in the regulation of *Fgf21* in BAT.

Interestingly, the gene expression levels of the pro-inflammatory chemokine *Ccl2* (MCP-1) negatively correlated with the sum of SPMs and with the sum of all Rvs and PDs classes (RvDs, RvEs, RvTs, RvDs_{n-3DPA}, PDs, and PDs_{n-3DPA}). Individual SPMs that negatively correlated with *Ccl2* included DHA and/or n-3 DPA-derived RvD1, RvD3, RvD5, RvD6, RvT1, RvT4, RvD5_{n-3DPA}, 10S,17S-diHDHA, 10S,17S-diHDPA, PD2_{n-3DPA}, MaR1, MaR2, 4,14-diHDHA, and 7S,14S-diHDPA. Despite a negative correlation was also found with the pro-inflammatory LTC_4 , all these observations suggest that the expression of this chemokine, which promotes the recruitment of M1 pro-inflammatory macrophages to adipose tissue, was clearly negatively related to the levels of SPMs.

Moreover, the mRNA expression of the anti-inflammatory cytokine *Il10* was negatively correlated with the sum of Pro-LMs and, accordingly, with the sum of LTBs, $cysLTs$, PGs, and TXs. Individual negative correlations were found for 5S,15S-diHETE, 5S,12S-diHETE, LTC_4 , PGE_2 , $PGF_{2\alpha}$ and TxB_2 . Although no correlations were found between *Il10*

and any of the individual LXs measured, a negative association was observed for the sum of LXs, suggesting a potential dual role for LOX-derived lipid mediators in the modulation of *Il10* mRNA levels, and vice versa. Despite IL-4 functions as an anti-inflammatory cytokine are well established, no associations were found between any SPM and this interleukin. Altogether, these data suggest strong associations of the analyzed lipid mediators with BAT function and inflammatory status, which were more significant for *Prdm16*, *Ccl2*, and *Il10* mRNA levels.

3.5 | Effects of aging, obesity, and long-term DHA supplementation on cold-induced BAT activation

Finally, we evaluated the changes in BAT activity in response to cold activation during aging and under obesogenic conditions, as well as the potential ability of DHA to prevent the decline in BAT activation. BAT activity in response to cold exposure was estimated by in vivo [^{18}F] FDG uptake MicroPET (Figure 8). PET analysis (coronal images, SUVmax value and ex vivo quantification of [^{18}F] FDG uptake in BAT depots)⁵⁴ revealed a clear decrease in BAT activation with aging, which was dramatically exacerbated in aged, obese groups. Besides the beneficial effects of DHA on genes and proteins regulating BAT development and function (*Prdm16* and UCP1), chronic dietary supplementation with this fatty acid was not able to reverse the impaired BAT response to cold observed in aged DIO mice (Figure 8A-C).

4 | DISCUSSION

Here, we describe for the first time BAT composition in n-3 PUFA-derived and AA-derived proresolving lipid mediators

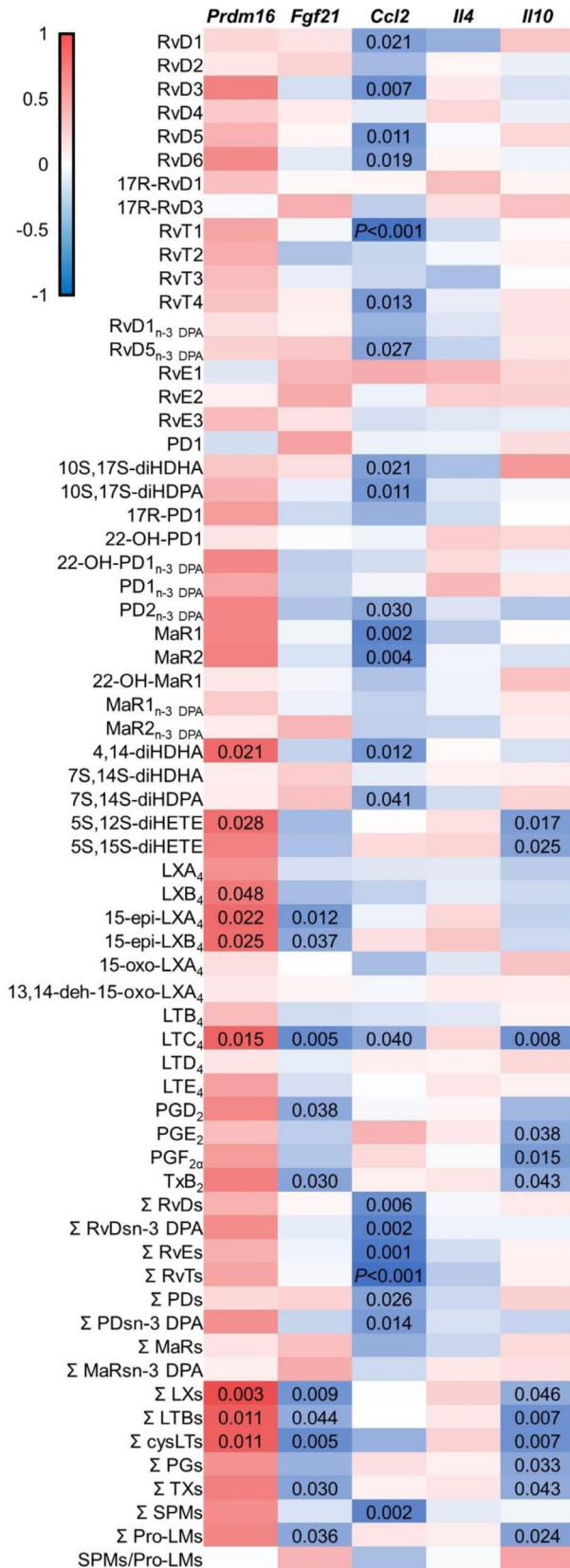


FIGURE 7 Heatmap showing Pearson's correlations of individualized lipid mediators and the sums of lipid mediator's classes with the expression of genes involved in BAT development, function, and inflammatory status (*Prdm6*, *Fgf21*, *Ccl2*, *Il10*, and *Il14*). Negative correlations are shown in blue and positive correlations are in red (see color scale). *P* value is indicated for significant correlations ($P < .05$)

in young control mice, along with their changes during aging, especially in obese mice and after chronic feeding with a DHA-enriched HFD.

Lipid mediator profiling studies of BAT revealed that the most abundant SPMs in CT mice at 2 months of age housed at room temperature were AA-derived LXs followed by DHA-derived MaRs and PDs. The most abundant AA-derived LXs pathway included 5S,15S-diHETE, 15-epi-LXA₄, and LXB₄, suggesting a potential role of these lipid mediators in the active BAT. A recent study has shown that LXA₄ and its precursor 15-HETE are among the major contributors differentiating BAT from WAT under thermoneutrality conditions.²⁹ Moreover, a study has suggested the relevance of the LXs pathway in BAT activity. Indeed, the overexpression of the arachidonate 5-lipoxygenase-activating protein (ALOX5AP), which is involved in the biosynthesis of LXs, increased LXA₄ production, upregulated UCP1, and thermogenesis resulting in protection against diet-induced obesity and insulin resistance in mice.⁵⁵ In our study, LXA₄ was also identified in BAT of young mice, but the levels were lower than those of LXB₄ or 15-epi-LXA₄, suggesting an undescribed role for these two AA-derived lipid mediators in BAT function. Interestingly, the levels of 15-epi-LXA₄, LXB₄, and LXA₄ were significantly decreased in BAT of aged DIO mice, in parallel with the dramatic drop in BAT activity as revealed by the lower UCP1 levels and especially the [¹⁸F]FDG uptake by this tissue. LXs were shown to be decreased in WAT from aging animals which also showed decreased resolution of inflammation.²² Moreover, a study has shown that aging is accompanied by a profound decrease in LXA₄ urine levels, especially from middle-aged adulthood to older adults.²¹

Concerning AA-derived lipid mediators, our study has also found that AA-derived prostaglandins (PGs: PGD₂, PGE₂ and PGF_{2α}) constitute the most abundant analyzed lipid mediators in BAT of young mice. In addition to their role in inflammation, AA-derived PGs are also involved in the regulation of cell proliferation and differentiation and energy metabolism.⁵⁶ Indeed, a study has shown that the COX-2-derived PG pathway seems to play a relevant role in controlling the differentiation of defined mesenchymal progenitors toward the phenotype of brown adipocytes.⁵⁷ Moreover, PGE₂ has been proposed to promote white-to-brown adipogenic differentiation.⁵⁸ In this way, the study of Garcia-Alonso et al⁵⁹ has shown that PGE₂ reduced inflammatory genes (IL-6 and

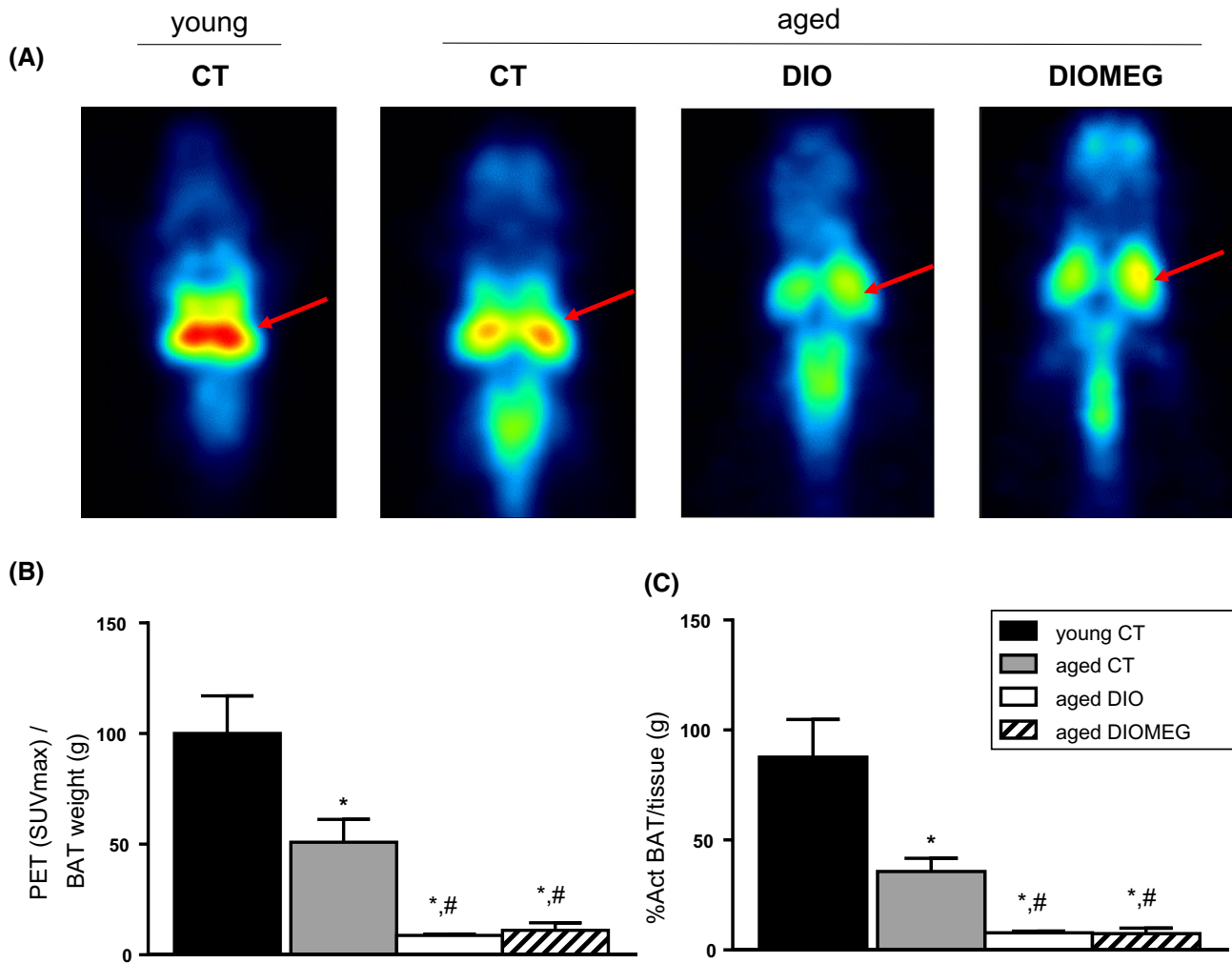


FIGURE 8 Cold-stimulated BAT activity is decreased with aging especially in obese mice, and it is not preserved by chronic DHA supplementation. A, BAT activity assessed by [^{18}F]FDG MicroPET in the four experimental groups. Mice were exposed for 1 hour at 4°C , prior injection of [^{18}F]FDG: coronal sections of mice. Red arrow: interscapular BAT pads. B, Maximum standardized uptake value (SUVmax/BAT weight) (g). C, Ex vivo quantification of [^{18}F]FDG uptake in BAT depots. (n = 4-5). Data are expressed as mean \pm SEM. * $P < .05$ vs young CT group; # $P < .05$ vs aged CT group

MCP-1) and induced the expression of brown markers (UCP1 and PRDM16) in WAT and adipocytes. Although PGE_2 levels were moderately reduced during aging in BAT, no significant changes were observed. In contrast, our study has revealed that the levels of $\text{PGF}_{2\alpha}$ were significantly inhibited in aged CT and DIO animals, suggesting that the drop in this eicosanoid could be involved in BAT reduced activity during aging. A study in humans has shown that serum 15-keto- $\text{PGF}_{2\alpha}$ is decreased, and correlates negatively with aging in nonobese humans.²⁰ However, the role for PGE_2 and $\text{PGF}_{2\alpha}$ on thermogenic adipocytes is controversial, since other study has shown that AA inhibits the browning process in human adipose tissue-derived mesenchymal stem cells (hMADS) adipocytes through the secretion of PGE_2 and $\text{PGF}_{2\alpha}$.⁶⁰ Moreover, PGE_2 and $\text{PGF}_{2\alpha}$ as well as 10S,17S-diHDHA (PDX) were also recently unraveled as one of the main lipid mediators that

contribute to differentiate BAT from WAT under thermoneutrality conditions.²⁹

Our study has also identified PDX as the most abundant DHA-derived PD in BAT of young mice that is reduced by aging especially in obese mice. PDX administration to obese diabetic mice improves insulin sensitivity by raising IL-6 skeletal muscle, without any impact on adipose tissue inflammation.⁶¹ However, the same authors found that PDX is present in WAT and promotes PPAR- γ transcriptional activity in *fat1* transgenic mice.⁶² Our current data suggest that PDX could play an uncharacterized role in BAT maintenance during aging.

DHA-derived MaR2 and 4S,14S-diHDHA are the most abundant molecules of the MaRs pathways, and both are significantly reduced during aging mainly in obese-aged mice. A similar trend was observed for MaR1 which was

less abundant in BAT of young mice. MaRs, biosynthesized through the 12-LOX pathway, are macrophage mediators with potent anti-inflammatory and proresolving actions.^{63,64} Previous studies from our group have demonstrated that MaR1 attenuates inflammation, improves insulin resistance, and restores metabolic pathways in adipocytes and in WAT of obese mice.^{26,65} MaR1 has been also shown to resolve aged-associated macrophage inflammation to improve bone regeneration.⁶⁶ However, the actions of MaR2 in brown/white adipose tissue are still unknown. Clària et al²³ found that 14-HDHA, a precursor of MaRs, was reduced in WAT of obese mice. Interestingly, Leiria et al⁵³ described that 14-HDHA was increased in BAT from female mice after 7 days of cold exposure compared to thermoneutrality conditions, and that this change occurred along with improved glucose uptake in BAT. This observation clearly suggests a role of the MaRs pathway in the regulation of BAT thermogenesis.

Although the abundance of Rvs in BAT was significantly lower than LXs, PDs, and MaRs, some of them showed relevant changes during obesity and aging. Thus, the levels of RvD6 and RvT1 were significantly lower in BAT of aged DIO mice. To the best of our knowledge, there is no previous data about the identification of these Rvs in adipose tissue or with changes in obesity. However, a metabolome study in human plasma identified RvD6 as a biomarker decreased in the aging process.²⁰ Although the effects of some Rvs such as RvD1 and RvD2 have been well characterized on the obese WAT,^{23,25,67} there is few information available about their effects on BAT. Interestingly, Pascoal et al⁶⁸ found that the intracerebroventricular administration of RvD2 promotes UCP1 and PGC1 α expression in BAT at doses of 3 ng, but not at 50 ng, which did not have any significant effect.

Few studies have analyzed the changes in BAT lipidomics during aging. A recent study using integrated metabolomics has found an altered lipid profile in BAT of an animal model of extreme longevity, the Ames dwarf mice, identifying increased levels of 5-HEPE, an n-3 PUFA metabolite, in BAT of these animals which exhibit increased thermogenesis.⁶⁹ This study reinforces that changes in BAT lipid signatures might account for the changes in BAT activity during aging.

In this sense, our study provides novel observations supporting that the decrease in BAT activity that occurs with aging, and especially in obesogenic conditions, could be related with a decrease in the abundance of proresolving lipid mediators in this tissue. However, the observations that the decrease in SPMs was much more pronounced in aged obese than in aged lean mice, suggests that the HFD feeding or obesity per se could be major determinants of SPMs reduction in BAT as compared to aging alone. Indeed, shorter periods of HFD-feeding or genetic obesity have been shown to reduce SPMs content in WAT.²⁴ Therefore, to better discriminate the effects of obesity and aging on BAT SPMs signature, it would be of interest to determine, in future studies, if high-fat

feeding in younger animals is able to alter the SPMs profile of BAT.

In this context, a recent study in human adipose tissue has revealed that the presence of active BAT is positively associated with an anti-inflammatory oxylipins/eicosanoids profile.⁷⁰ Similarly, EPA and DHA have been recently associated with the levels of BAT activity in humans.⁷¹ A lipidomic analysis of BAT in young mice showed that phospholipids and free fatty acids were more abundant in BAT than in WAT, and that phospholipids in BAT were mostly composed of PUFAs, especially DHA.⁷²

Our study shows that chronic dietary supplementation with DHA was able to reverse the drop in the sum of SPMs observed in BAT of aged DIO mice, reaching even values significantly higher than those found in BAT of young mice. This occurs in parallel with the upregulation of UCP1 and *Prdm16* and with a drop of pro-inflammatory genes such as *Ccl2* in BAT of DHA-supplemented aged DIOMEG mice. Several studies in cultured brown adipocytes have demonstrated the ability of n-3 PUFA, mainly EPA to induce brown development and thermogenic functions.^{36,73,74} Moreover, several studies in mice have shown that dietary supplementation with n-3 PUFA-rich fish oil (8-12 weeks) induce UCP1 expression in BAT.^{35,74,75}

Our current data suggest that DHA supplementation could be an approach to restore the deleterious effects of aging and obesity on key genes and proteins involved in BAT development and function, and that these DHA's actions are mediated through the increase in the production of all types of n-3 PUFA-derived SPMs (PDs, MaRs, and Rvs). Previous studies have shown that DHA administration led to an increase in SPMs and oxylipins in WAT both in animal models of obesity^{24,26,32} and obese subjects.³³ Such increase in SPMs occurred along with decreased time for resolution of inflammation, decreased macrophages infiltration, and induction of an anti-inflammatory phenotype. Our current data also show a relationship between the changes in SPMs and the expression of pro-inflammatory and anti-inflammatory genes in BAT, suggesting a causative correlation between both facts. Only two recent investigations analyzed the effects of n-3 PUFA supplementation on BAT activity and its relation to SPMs. Colson et al⁷⁶ recently compared the effects of 12 weeks feeding with a isocaloric diet enriched with n-6 PUFA or n-3 PUFA on oxylipin synthesis and adipose tissue inflammatory markers, observing that diet-enrichment with n-3 PUFAs induced an increase in oxylipins derived from EPA and DHA, without affecting the n-6 AA-derived metabolites. However, the levels of the final metabolites of oxylipins-pathway (PDX, MaR1, RvD1, RvD2, and RvE1) were barely or non-detected in this study as compared to our current data. However, DHA-derived LOX pathway 17-HDHA and 14-HDHA were detectable and increased with the n-3-PUFA-enriched diet.

In parallel, an increase in M2 macrophage markers was observed without changes in pro-inflammatory (*Il1 β* , *Il2*, and *Tnfa*) or anti-inflammatory (*Il4* and *Il10*) gene markers in BAT. Nevertheless, mice were younger (22 weeks) and were housed in thermoneutrality conditions ($28 \pm 2^\circ\text{C}$), without a high-fat dietary challenge and with a different dietary content of n-3 PUFA. Interestingly, Ghandour et al⁷⁷ found that dietary n-3 PUFA supplementation increased UCP1 in BAT and reduced the AA-derived TXB₂. Our current data also show that DHA-supplementation increased UCP1 in BAT and reduced TXB₂ levels in aged DIO mice.

We also tested if the increase in UCP1 and *Prdm16* along with the rise in n-3 PUFA-derived SPMs was associated with an improved BAT activity in response to cold-stimuli. Intriguingly, the MicroPET studies revealed that the drop in BAT [¹⁸F]FDG uptake observed in aged DIO mice was not recovered by chronic DHA supplementation, suggesting that other mechanisms involved in the cold-induced BAT activation impaired by obesity and aging are not restored by DHA supplementation. Sympathetic tone plays a key role in cold-induced BAT thermogenesis. Indeed, denervation of BAT in cold-exposed animals highlights the importance of its sympathetic innervation for thermogenic responses.⁷⁸ Moreover, an altered sympathetic tone has been hypothesized as a possible cause for the decrease in BAT recruitment in aging.⁷⁹ Importantly, a study has found that reduced cold-induced thermogenesis correlate with norepinephrine turnover rates that were reduced in older female rats, but not in male.⁴¹ Our study has been carried out in female mice and, therefore, we hypothesized that the defective cold response in aged DIO mice could be secondary to altered sympathetic tone. In this way, a study showed that fish oil intake was not able to induce UCP1 expression in transient receptor potential vanilloid 1 (TRPV1) knockout mice, suggesting that n-3 PUFA could induce UCP1 upregulation in BAT via the sympathetic nervous system.³⁵

Another hypothesis for the lack of relevant effects on BAT activity beside the increase in SPMs after chronic DHA supplementation could be that obesity and aging might also impair the expression/function of SPMs receptors in BAT. No study has investigated this issue, but others have found decreased expression of the receptors ALX/FPR2, Chemerin Receptor 23 (ChemR23) and G protein-coupled receptor 32 (GPR32) in WAT depots from obese mice and humans compared to lean.²³ Moreover, the knockout mice for *ChemR23* and *ALX/FPR2* developed obesity and, over the course of 12 months, cardiometabolic dysfunctions typical of aging.^{80,81} Future studies should focus in characterizing the changes in the expression and function of the SPMs receptors and SPMs signaling in BAT during aging and obesity, as they could also be relevant for the changes in BAT activation and for the efficient response to these metabolically active pro-resolving molecules.

In contrast to the rise observed for n-3 PUFA-derived SPMs, DHA supplementation was not able to reverse the dramatic drop in LXs observed in BAT of obese-aged mice. Taken into account the previously described thermogenic properties of the LXs pathway activation in BAT,⁵⁵ our data suggest that LXs could be important in mediating the loss of BAT activity during aging and the cold-response capacity in this tissue. Indeed, we have observed a correlation between *Prdm16* and the sum of LXs in BAT. However, further studies are needed to test this possibility.

Furthermore, previous studies have suggested sex differences in BAT lipidomic profile.⁷² Moreover, differential responses in BAT proteome and function have been observed between male and female after dietary interventions with both high-fat feeding or caloric restriction.^{40,82,83} A limitation of our current study is that it has been conducted only in female mice. Therefore, it would be of high relevance to carry out further comparative studies of SPMs changes in aged obese male and female mice in future studies. Another interesting issue to be addressed in future trials is the characterization of the changes in SPMs in BAT under thermoneutrality and cold exposure conditions.

In summary, our lipid mediator profiling analysis revealed for the first time that obesity promotes the decay in n-3 PUFA and AA-derived SPMs that occurs during aging in BAT, which relates with reduced markers of BAT function. Although long-term DHA supplementation prevented the drop in n-3 PUFA-derived SPMs in BAT, and improved BAT biomarkers, it was not able to restore the impaired response to cold exposure observed in obese-aged mice. Our study highlights the relevance to carry out further research to better characterize the physiological role of specific SPMs on BAT development and function as they could be potential therapeutic targets to modulate this thermogenic tissue.

ACKNOWLEDGMENTS

The authors thank Asunción Redín and Marga Ecay for her valuable technical support on this project. We also thank Dr. S. Lorente-Cebrián, Dr. P. Lostao and Dr. P. González-Muniesa (University of Navarra) for helpful scientific discussions/advice.

CONFLICT OF INTEREST


The authors declare no conflict of interest.

AUTHOR CONTRIBUTIONS

M.J. Moreno-Aliaga designed research, raised grant, and coordinated the project; E. Félix-Soriano, E. Gil-Iturbe, and N. Sáinz conducted the animal research; M. Collantes design and performed the MicroPET studies; L. Ly and J. Dalli carried out the lipidomic studies; E. Félix-Soriano, N. Sáinz, M. Fernández-Galilea, and R. Castilla-Madrigrá conducted the laboratory

research; E. Félix-Soriano and L. Ly performed the statistical analyses; E. Félix-Soriano and M.J. Moreno-Aliaga wrote the manuscript; all authors critically reviewed the manuscript.

ORCID

Elisa Félix-Soriano  <https://orcid.org/0000-0003-4633-1289>

Neira Sáinz  <https://orcid.org/0000-0003-0298-3031>

Eva Gil-Iturbe  <https://orcid.org/0000-0002-4046-5756>

María Collantes  <https://orcid.org/0000-0003-1162-1470>

Marta Fernández-Galilea  <https://orcid.org/0000-0002-4822-3188>

Rosa Castilla-Madrigal  <https://orcid.org/0000-0002-7610-1516>

Jesmond Dalli  <https://orcid.org/0000-0001-6328-3640>

María J. Moreno-Aliaga  <https://orcid.org/0000-0002-2018-6434>

REFERENCES

- Villarroya F, Cereijo R, Gavalda-Navarro A, Villarroya J, Giralt M. Inflammation of brown/beige adipose tissues in obesity and metabolic disease. *J Intern Med.* 2018;284(5):492-504. <https://doi.org/10.1111/joim.12803>.
- Chondronikola M, Volpi E, Borsheim E, et al. Brown adipose tissue improves whole-body glucose homeostasis and insulin sensitivity in humans. *Diabetes.* 2014;63(12):4089-4099. <https://doi.org/10.2337/db14-0746>.
- Bartelt A, Bruns OT, Reimer R, et al. Brown adipose tissue activity controls triglyceride clearance. *Nat Med.* 2011;17(2):200-206. <https://doi.org/10.1038/nm.2297>.
- Villarroya F, Cereijo R, Villarroya J, Giralt M. Brown adipose tissue as a secretory organ. *Nat Rev Endocrinol.* 2017;13(1):26-35. <https://doi.org/10.1038/nrendo.2016.136>.
- Fuse S, Sugimoto M, Kurosawa Y, et al. Relationships between plasma lipidomic profiles and brown adipose tissue density in humans. *Int J Obes.* 2020;44(6):1387-1396. <https://doi.org/10.1038/s41366-020-0558-y>.
- Hanssen MJW, Wierts R, Hoeks J, et al. Glucose uptake in human brown adipose tissue is impaired upon fasting-induced insulin resistance. *Diabetologia.* 2015;58(3):586-595. <https://doi.org/10.1007/s00125-014-3465-8>.
- Matsushita M, Yoneshiro T, Aita S, Kameya T, Sugie H, Saito M. Impact of brown adipose tissue on body fatness and glucose metabolism in healthy humans. *Int J Obes.* 2014;38(6):812-817. <https://doi.org/10.1038/ijo.2013.206>.
- Saito M, Okamatsu-Ogura Y, Matsushita M, et al. High incidence of metabolically active brown adipose tissue in healthy adult humans: effects of cold exposure and adiposity. *Diabetes.* 2009;58(7):1526-1531. <https://doi.org/10.2337/db09-0530>.
- Soundarrajan M, Deng J, Kwasny M, et al. Activated brown adipose tissue and its relationship to adiposity and metabolic markers: an exploratory study. *Adipocyte.* 2020;9(1):87-95. <https://doi.org/10.1080/21623945.2020.1724740>.
- Loh RKC, Kingwell BA, Carey AL. Human brown adipose tissue as a target for obesity management; beyond cold-induced thermogenesis. *Obes Rev.* 2017;18(11):1227-1242. <https://doi.org/10.1111/obr.12584>.
- Fuse S, Nirengi S, Amagasa S, et al. Brown adipose tissue density measured by near-infrared time-resolved spectroscopy in Japanese, across a wide age range. *J Biomed Opt.* 2018;23(6):1-9. <https://doi.org/10.1117/1.jbo.23.6.065002>.
- Cypess AM, Lehman S, Williams G, et al. Identification and importance of brown adipose tissue in adult humans. *N Engl J Med.* 2009;360(15):1509-1517. <https://doi.org/10.1056/NEJMoa0810780>.
- Moreno-Aliaga MJ, Villarroya F. Nutritional and metabolic regulation of brown and beige adipose tissues. *J Physiol Biochem.* 2020;76(2):181-184. <https://doi.org/10.1007/s13105-020-00745-1>.
- Serhan CN, Chiang N, Dalli J. New pro-resolving n-3 mediators bridge resolution of infectious inflammation to tissue regeneration. *Mol Aspects Med.* 2018;64:1-17. <https://doi.org/10.1016/j.mam.2017.08.002>.
- Livshits G, Kalinkovich A. Inflammaging as a common ground for the development and maintenance of sarcopenia, obesity, cardiomyopathy and dysbiosis. *Ageing Res Rev.* 2019;56:100980. <https://doi.org/10.1016/j.arr.2019.100980>.
- Wu D, Ren Z, Pae M, et al. Aging up-regulates expression of inflammatory mediators in mouse adipose tissue. *J Immunol.* 2007;179(7):4829-4839. <https://doi.org/10.4049/jimmunol.179.7.4829>.
- Pérez LM, Pareja-Galeano H, Sanchis-Gomar F, Emanuele E, Lucia A, Gálvez BG. 'Adipaging': ageing and obesity share biological hallmarks related to a dysfunctional adipose tissue. *J Physiol.* 2016;594(12):3187-3207. <https://doi.org/10.1113/JP271691>.
- Fitzgibbons TP, Kogan S, Aouadi M, Hendricks GM, Straubhaar J, Czech MP. Similarity of mouse perivascular and brown adipose tissues and their resistance to diet-induced inflammation. *Am J Physiol Heart Circ Physiol.* 2011;301(4):1425-1437. <https://doi.org/10.1152/ajpheart.00376.2011>.
- Sakamoto T, Nitta T, Maruno K, et al. Macrophage infiltration into obese adipose tissues suppresses the induction of UCPI level in mice. *Am J Physiol Endocrinol Metab.* 2016;310(8):E676-E687. <https://doi.org/10.1152/ajpendo.00028.2015>.
- Jové M, Maté I, Naudí A, et al. Human aging is a metabolome-related matter of gender. *Journals Gerontol Ser A Biol Sci Med Sci.* 2016;71(5):578-585. <https://doi.org/10.1093/gerona/glv074>.
- Gangemi S, Pescara L, D'Urbano E, et al. Aging is characterized by a profound reduction in anti-inflammatory lipoxin A4 levels. *Exp Gerontol.* 2005;40(7):612-614. <https://doi.org/10.1016/j.exger.2005.04.004>.
- Arnardottir HH, Dalli J, Colas RA, Shinohara M, Serhan CN. Aging delays resolution of acute inflammation in mice: reprogramming the host response with novel nano-proresolving medicines. *J Immunol.* 2014;193(8):4235-4244. <https://doi.org/10.4049/jimmunol.1401313>.
- Clària J, Dalli J, Yacoubian S, Gao F, Serhan CN. Resolvin D1 and resolvin D2 govern local inflammatory tone in obese fat. *J Immunol.* 2012;189(5):2597-2605. <https://doi.org/10.4049/jimmunol.1201272>.
- Neuhofer A, Zeyda M, Mascher D, et al. Impaired local production of proresolving lipid mediators in obesity and 17-HDHA as a potential treatment for obesity-associated inflammation. *Diabetes.* 2013;62(6):1945-1956. <https://doi.org/10.2337/db12-0828>.
- Hellmann J, Tang Y, Kosuri M, Bhatnagar A, Spite M. Resolvin D1 decreases adipose tissue macrophage accumulation and improves insulin sensitivity in obese-diabetic mice. *FASEB J.* 2011;25(7):2399-2407. <https://doi.org/10.1096/fj.10-178657>.

26. Martínez-Fernández L, González-Muniesa P, Laiglesia LM, et al. Maresin 1 improves insulin sensitivity and attenuates adipose tissue inflammation in ob/ob and diet-induced obese mice. *FASEB J*. 2017;31(5):2135-2145. <https://doi.org/10.1096/fj.201600859R>.
27. Laiglesia LM, Lorente-Cebrián S, Martínez-Fernández L, et al. Maresin 1 mitigates liver steatosis in ob/ob and diet-induced obese mice. *Int J Obes*. 2018;42(3):572-579. <https://doi.org/10.1038/ijo.2017.226>.
28. Grzybek M, Palladini A, Alexaki VI, et al. Comprehensive and quantitative analysis of white and brown adipose tissue by shotgun lipidomics. *Mol Metab*. 2019;22:12-20. <https://doi.org/10.1016/j.molmet.2019.01.009>.
29. Dieckmann S, Maurer S, Fromme T, et al. Fatty acid metabolite profiling reveals oxylipins as markers of brown but not white adipose tissue. *Front Endocrinol*. 2020;11:73. <https://doi.org/10.3389/fendo.2020.00073>.
30. Calder PC. Eicosapentaenoic and docosahexaenoic acid derived specialised pro-resolving mediators: concentrations in humans and the effects of age, sex, disease and increased omega-3 fatty acid intake. *Biochimie*. 2020;178:105-123. <https://doi.org/10.1016/j.biochi.2020.08.015>.
31. Ostermann AI, West AL, Schoenfeld K, et al. Plasma oxylipins respond in a linear dose-response manner with increased intake of EPA and DHA: results from a randomized controlled trial in healthy humans. *Am J Clin Nutr*. 2019;109(5):1251-1263. <https://doi.org/10.1093/ajcn/nqz016>.
32. González-Pérez A, Horrillo R, Ferré N, et al. Obesity-induced insulin resistance and hepatic steatosis are alleviated by omega-3 fatty acids: a role for resolvins and protectins. *FASEB J*. 2009;23(6):1946-1957. <https://doi.org/10.1096/fj.08-125674>.
33. Itariu BK, Zeyda M, Hochbrugger EE, et al. Long-chain n-3 PUFAs reduce adipose tissue and systemic inflammation in severely obese nondiabetic patients: a randomized controlled trial. *Am J Clin Nutr*. 2012;96(5):1137-1149. <http://doi.org/10.3945/ajcn.112.037432>.
34. Bargut TCL, Martins FF, Santos LP, Aguila MB, Mandarim-de-Lacerda CA. Administration of eicosapentaenoic and docosahexaenoic acids may improve the remodeling and browning in subcutaneous white adipose tissue and thermogenic markers in brown adipose tissue in mice. *Mol Cell Endocrinol*. 2019;482:18-27. <https://doi.org/10.1016/j.mce.2018.12.003>.
35. Kim M, Goto T, Yu R, et al. Fish oil intake induces UCP1 upregulation in brown and white adipose tissue via the sympathetic nervous system. *Sci Rep*. 2015;5:18013. <https://doi.org/10.1038/srep18013>.
36. Quesada-López T, Cereijo R, Turatsinze J-V, et al. The lipid sensor GPR120 promotes brown fat activation and FGF21 release from adipocytes. *Nat Commun*. 2016;17:13479. <https://doi.org/10.1038/ncomms13479>.
37. Fernández-Galilea M, Félix-Soriano E, Colón-Mesa I, Escoté X, Moreno-Aliaga MJ. Omega-3 fatty acids as regulators of brown/beige adipose tissue: from mechanisms to therapeutic potential. *J Physiol Biochem*. 2019;76(2):251-257. <https://doi.org/10.1007/s13105-019-00720-5>.
38. Yang J, Sáinz N, Félix-Soriano E, et al. Effects of long-term DHA supplementation and physical exercise on non-alcoholic fatty liver development in obese aged female mice. *Nutrients*. 2021;13(2):501. <https://doi.org/10.3390/nu13020501>.
39. Roca P, Rodríguez AM, Oliver P, et al. Brown adipose tissue response to cafeteria diet-feeding involves induction of the UCP2 gene and is impaired in female rats as compared to males. *Pflugers Arch Eur J Physiol*. 1999;438(5):628-634. <https://doi.org/10.1007/s004249900107>.
40. Valle A, García-Palmer F, Oliver J, Roca P. Sex differences in brown adipose tissue thermogenic features during caloric restriction. *Cell Physiol Biochem*. 2007;19(1-4):195-204. <https://doi.org/10.1159/000099207>.
41. McDonald RB, Horwitz BA. Brown adipose tissue thermogenesis during aging and senescence. *J Bioenerg Biomembr*. 1999;31(5):507-516. <https://doi.org/10.1023/A:1005404708710>.
42. Moreno-Aliaga MJ, Pérez-Echarri N, Marcos-Gómez B, et al. Cardiostrophin-1 is a key regulator of glucose and lipid metabolism. *Cell Metab*. 2011;14(2):242-253. <https://doi.org/10.1016/j.cmet.2011.05.013>.
43. Becerril S, Rodríguez A, Catalán V, et al. Deletion of inducible nitric-oxide synthase in leptin-deficient mice improves brown adipose tissue function. *PLoS ONE*. 2010;5(6):e10962. <https://doi.org/10.1371/journal.pone.0010962>.
44. Gomez EA, Colas RA, Souza PR, et al. Blood pro-resolving mediators are linked with synovial pathology and are predictive of DMARD responsiveness in rheumatoid arthritis. *Nat Commun*. 2020;11(1):5420. <https://doi.org/10.1038/s41467-020-19176-z>.
45. Colas RA, Gomez EA, Dalli J. Methodologies and procedures employed in the identification and quantitation of lipid mediators via LC-MS/MS. *Res Sq*. Published online 2020:1-16. <https://doi.org/10.21203/RS.3.PEX-1147/V1>.
46. Dalli J, Colas RA, Walker ME, Serhan CN. Lipid mediator metabolomics via LC-MS/MS profiling and analysis. *Methods Mol Biol*. 2018;1730:59-72. https://doi.org/10.1007/978-1-4939-7592-1_4.
47. Gil-Iturbe E, Félix-Soriano E, Sáinz N, et al. Effect of aging and obesity on GLUT12 expression in small intestine, adipose tissue, muscle and kidney, and its regulation by docosahexaenoic acid and exercise in mice. *Appl Physiol Nutr Metab*. 2020;45(9):957-967. <https://doi.org/10.1139/apnm-2019-0721>.
48. Livak KJ, Schmittgen TD. Analysis of relative gene expression data using real-time quantitative PCR and the 2(-Delta Delta C(T)) method. *Methods*. 2001;25(4):402-408. <https://doi.org/10.1006/meth.2001.1262>.
49. Harms M, Ishibashi J, Wang W, et al. Prdm16 is required for the maintenance of brown adipocyte identity and function in adult mice. *Cell Metab*. 2014;19(4):593-604. <https://doi.org/10.1016/j.cmet.2014.03.007>.
50. Fisher FM, Chui PC, Antonellis PJ, et al. Obesity is a fibroblast growth factor 21 (FGF21)-resistant state. *Diabetes*. 2010;59(11):2781-2789. <https://doi.org/10.2337/db10-0193>.
51. Villarroja F, Cereijo R, Villarroja J, Gavalda-Navarro A, Giral M. Toward an understanding of how immune cells control brown and beige adipobiology. *Cell Metab*. 2018;27(5):954-961. <https://doi.org/10.1016/j.cmet.2018.04.006>.
52. Lynes MD, Leiria LO, Lundh M, et al. The cold-induced lipokine 12,13-diHOME promotes fatty acid transport into brown adipose tissue. *Nat Med*. 2017;23(5):631-637. <https://doi.org/10.1038/nm.4297>.
53. Leiria LO, Wang C-H, Lynes MD, et al. 12-Lipoxygenase regulates cold adaptation and glucose metabolism by producing the omega-3 lipid 12-HEPE from brown fat. *Cell Metab*. 2019;30(4):768-783. <https://doi.org/10.1016/j.cmet.2019.07.001>.
54. Corrales P, Vivas Y, Izquierdo-Lahuerta A, et al. Long-term caloric restriction ameliorates deleterious effects of aging on white and brown adipose tissue plasticity. *Aging Cell*. 2019;18(3):e12948. <https://doi.org/10.1111/acer.12948>.

55. Elias I, Ferré T, Vilà L, et al. ALOX5AP overexpression in adipose tissue leads to LXA4 production and protection against diet-induced obesity and insulin resistance. *Diabetes*. 2016;65(8):2139-2150. <https://doi.org/10.2337/db16-0040>.
56. Chan PC, Liao MT, Hsieh PS. The dualistic effect of COX-2-mediated signaling in obesity and insulin resistance. *Int J Mol Sci*. 2019;20(13):3115. <https://doi.org/10.3390/ijms20133115>.
57. Madsen L, Pedersen LM, Lillefosse HH, et al. UCP1 induction during recruitment of brown adipocytes in white adipose tissue is dependent on cyclooxygenase activity. *PLoS ONE*. 2010;5(6):e11391. <https://doi.org/10.1371/journal.pone.0011391>.
58. García-Alonso V, López-Vicario C, Titos E, et al. Coordinate functional regulation between microsomal prostaglandin e synthase-1 (mPGES-1) and peroxisome proliferator-activated receptor γ (PPAR γ) in the conversion of white-to-brown adipocytes. *J Biol Chem*. 2013;288(39):28230-28242. <https://doi.org/10.1074/jbc.M113.468603>.
59. García-Alonso V, Titos E, Alcaraz-Quiles J, et al. Prostaglandin E2 exerts multiple regulatory actions on human obese adipose tissue remodeling, inflammation, adaptive thermogenesis and lipolysis. *PLoS ONE*. 2016;11(4):e0153751. <https://doi.org/10.1371/journal.pone.0153751>.
60. Pisani DF, Ghandour RA, Beranger GE, et al. The ω 6-fatty acid, arachidonic acid, regulates the conversion of white to brite adipocyte through a prostaglandin/calcium mediated pathway. *Mol Metab*. 2014;3(9):834-847. <https://doi.org/10.1016/j.molmet.2014.09.003>.
61. White PJ, St-Pierre P, Charbonneau A, et al. Protectin DX alleviates insulin resistance by activating a myokine-liver gluco-regulatory axis. *Nat Med*. 2014;20(6):664-669. <https://doi.org/10.1038/nm.3549>.
62. White PJ, Mitchell PL, Schwab M, et al. Transgenic ω -3 PUFA enrichment alters morphology and gene expression profile in adipose tissue of obese mice: potential role for protectins. *Metabolism*. 2015;64(6):666-676. <https://doi.org/10.1016/j.metabol.2015.01.017>.
63. Serhan CN, Yang R, Martinod K, et al. Maresins: Novel macrophage mediators with potent anti-inflammatory and pro-resolving actions. *J Exp Med*. 2009;206(1):15-23. <https://doi.org/10.1084/jem.20081880>.
64. Deng B, Wang C-W, Arnardottir HH, et al. Maresin biosynthesis and identification of maresin 2, a new anti-inflammatory and pro-resolving mediator from human macrophages. *PLoS ONE*. 2014;9(7):e102362. <https://doi.org/10.1371/journal.pone.0102362>.
65. Laiglesia LM, Lorente-Cebrián S, López-Yoldi M, et al. Maresin 1 inhibits TNF-alpha-induced lipolysis and autophagy in 3T3-L1 adipocytes. *J Cell Physiol*. 2018;233(3):2238-2246. <https://doi.org/10.1002/jcp.26096>.
66. Huang R, Vi L, Zong X, Baht GS. Maresin 1 resolves aged-associated macrophage inflammation to improve bone regeneration. *FASEB J*. 2020;34(10):13521-13532. <https://doi.org/10.1096/fj.202001145R>.
67. Titos E, Rius B, López-Vicario C, et al. Signaling and immunoresolving actions of resolvin D1 in inflamed human visceral adipose tissue. *Physiol Behav*. 2016;176(1):139-148. <https://doi.org/10.1016/j.physbeh.2017.03.040>.
68. Pascoal LB, Bombassaro B, Ramalho AF, et al. Resolvin RvD2 reduces hypothalamic inflammation and rescues mice from diet-induced obesity. *J Neuroinflammation*. 2017;14(1):5. <https://doi.org/10.1186/s12974-016-0777-2>.
69. Darcy J, Fang Y, McFadden S, et al. Integrated metabolomics reveals altered lipid metabolism in adipose tissue in a model of extreme longevity. *GeroScience*. 2020;42(6):1527-1546. <https://doi.org/10.1007/s11357-020-00221-0>.
70. Kulterer OC, Niederstaetter L, Herz CT, et al. The presence of active brown adipose tissue determines cold-induced energy expenditure and oxylipin profiles in humans. *J Clin Endocrinol Metab*. 2020;105(7):2203-2216. <https://doi.org/10.1080/2331186X.2019.1662162>.
71. Xiang AS, Giles C, Loh RKC, et al. Plasma docosahexaenoic acid and eicosapentaenoic acid concentrations are positively associated with brown adipose tissue activity in humans. *Metabolites*. 2020;10(10):388. <https://doi.org/10.3390/metabo10100388>.
72. Hoene M, Li J, Häring HU, Weigert C, Xu G, Lehmann R. The lipid profile of brown adipose tissue is sex-specific in mice. *Biochim Biophys Acta Mol Cell Biol Lipids*. 2014;1841(10):1563-1570. <https://doi.org/10.1016/j.bbalip.2014.08.003>.
73. Fleckenstein-Elsen M, Dinnies D, Jelenik T, Roden M, Romacho T, Eckel J. Eicosapentaenoic acid and arachidonic acid differentially regulate adipogenesis, acquisition of a brite phenotype and mitochondrial function in primary human adipocytes. *Mol Nutr Food Res*. 2016;60(9):2065-2075. <https://doi.org/10.1002/mnfr.20150892>.
74. Kim J, Okla M, Erickson A, Carr T, Natarajan SK, Chung S. Eicosapentaenoic acid potentiates brown thermogenesis through FFAR4-dependent up-regulation of miR-30b and miR-378. *J Biol Chem*. 2016;291(39):20551-20562. <https://doi.org/10.1074/jbc.M116.721480>.
75. Bargut TCL, Silva-e-Silva ACAG, Souza-Mello V, Mandarim-de-Lacerda CA, Aguila MB. Mice fed fish oil diet and upregulation of brown adipose tissue thermogenic markers. *Eur J Nutr*. 2016;55(1):159-169. <https://doi.org/10.1007/s00394-015-0834-0>.
76. Colson C, Ghandour R, Dufies O, et al. Diet supplementation in ω 3 polyunsaturated fatty acid favors an anti-inflammatory basal environment in mouse adipose tissue. *Nutrients*. 2019;11(2):438. <https://doi.org/10.3390/nu11020438>.
77. Ghandour RA, Colson C, Giroud M, et al. Impact of dietary ω 3 polyunsaturated fatty acid supplementation on brown and brite adipocyte function. *J Lipid Res*. 2018;59(3):452-461. <https://doi.org/10.1194/jlr.M081091>.
78. Bartness TJ, Vaughan CH, Song CK. Sympathetic and sensory innervation of brown adipose tissue. *Int J Obes*. 2010;34(S1):S36-S42. <https://doi.org/10.1038/ijo.2010.182>.
79. Graja A, Schulz TJ. Mechanisms of aging-related impairment of brown adipocyte development and function. *Gerontology*. 2015;61(3):211-217. <https://doi.org/10.1159/000366557>.
80. Rouger L, Denis GR, Luangsay S, Parmentier M. ChemR23 knockout mice display mild obesity but no deficit in adipocyte differentiation. *J Endocrinol*. 2013;219(3):279-289. <https://doi.org/10.1530/JOE-13-0106>.
81. Tourki B, Kain V, Pullen AB, et al. Lack of resolution sensor drives age-related cardiometabolic and cardiorenal defects and impedes inflammation-resolution in heart failure. *Mol Metab*. 2020;31:138-149. <https://doi.org/10.1016/j.molmet.2019.10.008>.
82. Choi DK, Oh TS, Choi J-W, et al. Gender difference in proteome of brown adipose tissues between male and female rats exposed to a high fat diet. *Cell Physiol Biochem*. 2011;28(5):933-948. <https://doi.org/10.1159/000335807>.

83. Valencak TG, Osterrieder A, Schulz TJ. Sex matters: the effects of biological sex on adipose tissue biology and energy metabolism. *Redox Biol.* 2017;12:806-813. <https://doi.org/10.1016/j.redox.2017.04.012>.

SUPPORTING INFORMATION

Additional Supporting Information may be found online in the Supporting Information section.

How to cite this article: Félix-Soriano E, Sáinz N, Gil-Iturbe E, et al. Changes in brown adipose tissue lipid mediator signatures with aging, obesity, and DHA supplementation in female mice. *The FASEB Journal.* 2021;35:e21592. <https://doi.org/10.1096/fj.202002531R>